2017

Unconditionally Energy Stable Numerical Schemes for Hydrodynamics Coupled Fluids Systems

Alexander Yuryevich Brylev
University of South Carolina

Unconditionally Energy Stable Numerical Schemes for
Hydrodynamics Coupled Fluids Systems

by

Alexander Yuryevich Brylev

Bachelor of Arts
Hamline University 2006

Master of Science
New Mexico State University 2011

_____

Submitted in Partial Fulfillment of the Requirements

for the Degree of Doctor of Philosophy in

Mathematics

College of Arts and Sciences

University of South Carolina

2017

Accepted by:

Xiaofeng Yang, Major Professor

Lili Ju, Committee Member

Zhu Wang, Committee Member

Xinfeng Liu, Committee Member

Dewei Wang, Outside Committee Member

Cheryl L. Addy, Vice Provost and Dean of the Graduate School

Acknowledgments

First of all, I would like to thank my thesis director, professor Xiaofeng Yang, for his support and guidance in writing this thesis. He held numerous office hours to work with me on it, was always prompt in answering e-mails and any questions I had about the research. This work wouldn't be possible without him. I also appreciate being funded by a research grant several times.

Next, I thank all my professors during my first two years at the University of South Carolina for helping me build the foundations I needed to be able to succeed in my project. Courses in Computational Mathematics (MATH 708 and MATH 709), taught by professors Lili Ju and Xiaofeng Yang, as well as Numerical Differential Equations (MATH 726) and Applied Mathematics (MATH 720 and MATH 721), taught by professor Hong Wang, turned out to be particularly valuable.

Finally, I would like to thank the department of Mathematics at the University of South Carolina for accepting me on a PhD program and providing me financial support in the form of teaching assistanship. I really enjoyed my work experience and it was great to be a part of the Gamecock family!

ABSTRACT

The thesis consists of two parts. In the first part we propose several second order in time, fully discrete, linear and nonlinear numerical schemes to solve the phase-field model of two-phase incompressible flows in the framework of finite element method. The schemes are based on the second order Crank-Nicolson method for time disretizations, projection method for Navier-Stokes equations, as well as several implicit-explicit treatments for phase-field equations. The energy stability, solvability, and uniqueness for numerical solutions of proposed schemes are further proved. Ample numerical experiments are performed to validate the accuracy and efficiency of the proposed schemes thereafter.

In the second part we consider the numerical approximations for the model of smectic-A liquid crystal flows. The model equation, that is derived from the variational approach of the de Gennes energy, is a highly nonlinear system that couples the incompressible Navier-Stokes equations and two nonlinear coupled second-order elliptic equations. Based on some subtle explicit-implicit treatments for nonlinear terms, we develop unconditionally energy stable, linear, decoupled time discretization scheme. We also rigorously prove that the proposed scheme obeys the energy dissipation law. Various numerical simulations are presented to demonstrate the accuracy and the stability thereafter.

TABLE OF CONTENTS

LIST OF TABLES

LIST OF FIGURES

CHAPTER 1

NUMERICAL ANALYSIS OF CERTAIN SCHEMES FOR PHASE FIELD MODELS OF TWO-PHASE INCOMPRESSIBLE FLOWS

1.1 INTRODUCTION

Interfacial problems have attracted much attention of scientists for over a century. A classical approach to dealing with such problems was to introduce a mesh with grid points on the interfaces which deforms according to the motion of the boundary. This method, however, had a drawback that large displacement or deformation of internal domains could cause computational issues such as mesh entaglement. To overcome this, sophisticated remeshing schemes were often times used [57]. Other methods which proved to work well were the volume-of-fluid (VOF) [48, 49], the front-tracking [40, 41] and the level-set [61, 78] fixed-grid methods, where the interfacial tension is represented as a body-force or bulk-stress spreading over a narrow region covering the interface. The VOF method is a numerical technique for tracking and locating the interface between the fluids using the marker function. The disadvatage of this method is in its difficulty maintaining the sharp interface between the fluids and the computation of the surface tension. The level-set method has improved the accuracy and, hence, the applicability of the VOF method. The problem with the level-set method occurs when one tries to use it in an advection field, for example, uniform or rotational velocity field. In this case the shape and size of the level set must be conserved, however, the method does not guarantee this, so the level set may get significantly distorted and vanish over several time steps. This requires

1

the use of high-order finite difference schemes, such as high-order essentially non-oscillatory (ENO) schemes [47], and even then, the feasibility of long-time simulations is questionable. To overcome this difficulty, more sophisticated methods have been designed, such as combinations of the level set method with tracing marker particles advected by the velocity field [60]. In the front-tracking method a separate front marks the interface but a fixed grid, only modified near the front to make a grid line follow the interface, is used for the fuid within each phase.

Phase-field or diffuse-interface model is another mathematical model for solving various interfacial problems. In recent years it has been successfully used to simulate dynamical processes in many fields and has become one of the major tools to study various systems arising from the energy-based variational formalism. The method employs an order parameter, called the phase field, and substitutes boundary conditions at the interface by the partial differential equation involving this new variable. The phase field is assigned distinct values on each phase (for example, -1 and 1) and a thin smooth transition layer marking the interface is defined as the set of all points where the phase field takes a certain value (for example, 0). Hence the dynamics of the interface can be simulated on a fixed grid without explicit interface tracking, which renders the diffuse interface method an attractive numerical approach to simulate free moving/deforming interfacial problems. Based on variational approaches, the governing system can be derived from the total free energy, which usually leads to some well-posed nonlinear partial differential equations. This makes it possible to carry out mathematical analysis and design numerical schemes which preserve the thermo-dynamically consistent dissipation law (energy-stable) at the discrete level. The preservation of such laws is critical for numerical methods to capture the correct long time dynamics.

The dynamics of phase field models can be described by either the Allen-Cahn equation [4] or the Cahn-Hilliard equation [8, 9] based on choices of Sobolev spaces

of the variational approach. In details, the Allen-Cahn equation is a second-order equation, which is easier to solve numerically but does not conserve the volume fraction, while the Cahn-Hilliard equation is a fourth-order equation which conserves the volume fraction but is relatively harder to solve numerically. Basically, the coarse-graining (macroscopic) process described by these two equations may undergo rapid changes near the interface, so the noncompliance of energy dissipation laws may lead to spurious numerical solutions if the grid and time step sizes are not carefully controlled [52, 36]. Thus, from the numerical point of view, people are particularly interested in designing simple, efficient and energy stable numerical schemes satisfying discrete energy dissipations laws.

There are several challenges to construct the efficient numerical schemes to solve the hydrodynamics coupled phase field model numerically, namely, i) the small interfacial width introduces tremendous amount of stiffness into the system ii) the nonlinear coupling between the phase variable and velocity due to the nonlinear convections and stresses, iii) the coupling between the velocity and pressure in the fluid momentum equation. It is by no means an easy task, in particular, the development of any efficient and accurate numerical schemes while maintaining the dissipative energy law.

It is remarkable that many attempts have been made in this direction recently (cf. a comprehensive summary in [65]. However, due to the complexity of the nonlinear convection terms and stresses in the system, most of developed schemes are either only first-order in time [44, 69, 67], or are nonlinear schemes which need some efficient iterative solvers [76, 15], or only focus on the no flow case [59, 77, 31], or unable to provide the stability analysis [17]. There are very few works with the focus on the development of the second order schemes for the hydrodynamics coupled phase field model.

Recently, in [32], a second order, unconditionally stable, semi-discrete scheme for

the hydrodynamics coupled Cahn-Hilliard phase field model was developed, which could be regarded as one of the limited successful efforts in the development of second order schemes. However, in [32], first, the schemes for the computation of the phase field variable are nonlinear thanks to the application of the convex splitting approach, thus one in turn needs some efficient iterative solvers. Second, the computation of the phase variable is always coupled with that of the velocity. Third, the proof of energy law is only for the time discretization case.

Therefore, the main objective of this paper is to develop some fully discrete, second-order, unconditionally stable schemes for the hydrodynamics coupled Cahn-Hilliard phase field model. We combine several approaches which have proved efficient for the phase equations and for the Navier-Stokes equations, namely, linear methods based on the Lagrangian multiplier approach (cf. [31]) and nonlinear methods based on the convex splitting approach (cf. [71, 32, 74, 22, 35, 75]) for the phase equations, and projection-type approaches [5, 43, 30] for the Navier-Stokes equations. For the proposed linear schemes, in spite of the fact that the computation of the phase field variable is still coupled with that of the velocity, one only needs to solve a linear elliptic system. This is extremely convenient since one can explicitly find the mass matrix for the linear system associated with the Finite Element method or Finite Difference method. In additions, we prove that the modified discrete energy law holds for all schemes. For the proposed nonlinear schemes, we prove rigorously its unconditional solvability for the fully discrete case. Ample numerical experiments are performed to validate the accuracy and efficiency thereafter.

The rest of the chapter is organized as follows. In Section 2, we present the whole model and the PDE energy law. In Section 3, we develop the numerical schemes and prove their unconditional stability and unconditionally unique solvability in the time discrete case. In section 4, the schemes are further discretized in time and space by mixed finite element approximation. Energy stabilities for fully discrete case are

proved. For nonlinear schemes, we further prove the solvability and uniqueness. Finally, we present some numerical experiments to validate our numerical schemes in Section 5. Some concluding remarks are presented in Section 6.

1.2 THE PDE SYSTEM AND ENERGY LAW.

We consider the phase field model for a mixture of two immiscible, incompressible fluids in a confined domain $\Omega \in R^d$, $(d = 2, 3)$. In order to label the two fluids, a phase variable (macroscopic labeling function) ϕ is introduced such that

$$\phi(x, t) = \begin{cases} 1 & \text{fluid I }, \\ -1 & \text{fluid II}, \end{cases} \tag{1.1}$$

with a smooth but thin transition layer, which is controlled by the parameter $\eta \ll 1$. The (equilibrium) configuration of this mixing layer, in the neighborhood of the level set $\Gamma_t = \{x : \phi(x, t) = 0\}$, is determined by the microscopic interactions between fluid molecules. For the isotropic interactions, the classical self consistent mean field theory (SCMFT) in statistical physics [10] yields the following Ginzburg-Landau type of Helmholtz free energy functional: where the first term contributes to the "hydro-philic" type (tendency of mixing) of interactions between the materials and the second part, the double well bulk energy $F(\phi) = \frac{(\phi^2-1)^2}{4\eta^2}$ represents the "hydro-phobic" type (tendency of separation) of interactions. As a consequence of the competition between the two types of interactions, the equilibrium configuration will include a diffusive interface with thickness proportional to the parameter η; and, as η approaches zero, we expect to recover the sharp interface separating the two different materials (cf., for instance, [80, 6, 21]).

The total energy of the hydrodynamic system is a sum of the kinetic energy E_k and the mixing energy E_{mix}:

$$E = E_k + E_{mix} = \int_\Omega \left(\frac{1}{2}|u|^2 + \lambda \left(\frac{|\nabla \phi|^2}{2} + F(\phi) \right) \right) dx, \tag{1.2}$$

5

where we assume the density of the two fluids are matched with $\rho = 1$ and u is the fluid velocity field. Assuming a generalized Fick's law that the mass flux be proportional to the gradient of the chemical potential [9, 8, 24, 55], one can derive the following (non-conserved) Allen-Cahn-Navier-Stokes (ACNS) system:

$$\phi_t + (u \cdot \nabla)\phi = -M\mu, \tag{1.3}$$

$$\mu = \frac{\delta E}{\delta \phi} = \lambda(-\Delta\phi + f(\phi)), \tag{1.4}$$

$$u_t + (u \cdot \nabla)u + \nabla p - \nu\Delta u = \mu\nabla\phi, \tag{1.5}$$

$$\nabla \cdot u = 0, \tag{1.6}$$

where $f(\phi) = F'(\phi) = \frac{(\phi^2-1)\phi}{\eta^2}$, p is the pressure, M is the relaxation or mobility parameter of the phase function, and ν is the viscosity parameter. If the variational derivative can be taken in the H^{-1}, leading to the (conserved) Cahn-Hilliard-Navier-Stokes (CHNS) equations,

$$\phi_t + (u \cdot \nabla)\phi = M\Delta\mu, \tag{1.7}$$

$$\mu = \lambda(-\Delta\phi + f(\phi)). \tag{1.8}$$

Throughout the paper, we assume the boundary conditions

$$u|_{\partial\Omega} = 0, \quad \partial_n\phi|_{\partial\Omega} = 0, \quad \partial_n\mu|_{\partial\Omega} = 0, \tag{1.9}$$

although all results are valid for periodic boundary conditions as well.

Since the above system was derived from the energetic variational formulation, it can be readily established that the total energy of the ACNS system ((1.3)–(1.6)), and CHNS system ((1.7)–(1.8)–(1.5)–(1.6)) are dissipative. More precisely, by taking the inner product of (1.3) with $\frac{\partial E}{\partial \phi}$, (1.5) with u, and then summing up these equalities, we obtain the following energy dissipation law for ACNS system:

$$\frac{d}{dt}E = -\int_\Omega \nu|\nabla u|^2 + M\left|\frac{\partial E}{\partial \phi}\right|^2 dx. \tag{1.10}$$

6

For CHNS system, by taking the L^2 inner product of (1.7) with μ, of (1.8) with ϕ_t, of (1.5) with u and summarize all equalities, we obtain

$$\frac{d}{dt}E = -\int_\Omega \left(\nu|\nabla u|^2 + M|\nabla\mu|^2 \right)dx. \tag{1.11}$$

However, for Allen-Cahn equation (1.3), the variational derivative $\frac{\delta E}{\delta\phi}$ involves the second order derivative, thus it is not suitable to use them as test functions in numerical approximations, making it difficult to prove the discrete energy dissipation law. Hence, it is a common practice to rewrite (1.5)-(1.6) as the following equivalent form [79, 37, 65].

$$u_t + u \cdot \nabla u - \nu\Delta u + \nabla p + \frac{1}{M}\Big(\phi_t + (u\cdot\nabla)\phi\Big)\nabla\phi = 0, \tag{1.12}$$

$$\nabla \cdot u = 0. \tag{1.13}$$

Now, by taking the L^2 inner product of (1.3) with ϕ_t and (1.12) with u, we obtain

$$\frac{d}{dt}E = -\int_\Omega \left(\nu|\nabla u|^2 + \frac{1}{M}|\dot\phi|^2 \right)dx, \quad \text{with} \quad \dot\phi = \phi_t + (u\cdot\nabla)\phi. \tag{1.14}$$

We emphasize that the above derivation is suitable in a finite dimensional approximation since test function ϕ_t is in the same subspaces as ϕ. Hence, it allows us to design numerical schemes which satisfy a discrete energy law.

Remark 1.2.1. • *It is well known that the solutions of the conserved Cahn–Hilliard phase equation, with suitable boundary conditions, satisfy the desired conservation property $\partial_t \int_\Omega \phi dx = 0$, which is not satisfied by the solutions of the non-conserved Allen–Cahn equation. In fact, one can add a scalar Lagrange multiplier in (1.3) to enforce this conservation property (cf. [79, 68]), or modify the free energy functional by adding a penalty term for volume, similar as [18]. Both ways will not introduce any mathematical or numerical difficulty, thus we shall not include it in the discussions below.*

- *For simplicity, we consider only in this paper the ACNS model (1.3)-(1.4)-(1.12)-(1.13). All theoretical proof can be generalized to the CHNS model (1.7)-(1.8)-(1.5)-(1.6) without any further difficulty. The detailed stability proof for CHNS system will be left to the interested readers.*

1.3 SECOND ORDER, SEMI-DISCRETE SCHEMES AND THEIR ENERGY STABILITY.

In this section, we construct several second order in time, semi-discrete schemes and present their energy stabilities. Let $\delta t > 0$ be a time step size and set $t^n = n\delta t$ for $0 \le n \le N = [T/\delta t]$. Without ambiguity, we denote by $(f(x), g(x)) = (\int_\Omega f(x)g(x)dx)^{\frac{1}{2}}$ the L^2 inner product between functions $f(x)$ and $g(x)$, by $\|f\| = (f, f)$ the L^2 norm of function $f(x)$.

1.3.1 THE LINEAR SCHEME.

We first construct a linear scheme based on a Lagrange multiplier approach in [31], where it is first developed to solve the Cahn-Hilliard equation without flow.

A function $q = \frac{\phi^2 - 1}{\eta^2}$ is introduced such that one can write $f(\phi) = q\phi$. It then follows that $q_t = \frac{2}{\eta^2}\phi\phi_t$. By using the variable q, the total energy can be written as

$$E = \int_\Omega \left(\frac{1}{2}|u|^2 + \lambda\left(\frac{|\nabla\phi|^2}{2} + \frac{\eta^2}{4}q^2\right) \right) dx. \tag{1.15}$$

It is remarkable that energy dissipation laws (1.11) and (1.14) still hold.

A linear scheme for solving the ACNS system is constructed as follows:

Given the initial conditions $\phi^0, u^0, q^0 = \frac{(\phi^0)^2 - 1}{\eta^2}$ and $p^0 = 0$, we compute ϕ^1, u^1, q^1 and p^1 by any first order methods (cf. [31, 69, 70]). Having computed $\phi^{n-1}, q^{n-1}, u^{n-1}, p^{n-1}$ and ϕ^n, q^n, u^n, p^n for $n \ge 1$, we compute $\phi^{n+1}, q^{n+1}, \tilde{u}^{n+1}, u^{n+1}, p^{n+1}$ by the following steps.

Step 1:

$$\dot{\phi}^{n+1} - \lambda M\left(\Delta\frac{\phi^{n+1} + \phi^n}{2} - \left(\frac{3}{2}\phi^n - \frac{1}{2}\phi^{n-1}\right)\frac{q^{n+1} + q^n}{2}\right) = 0, \qquad (1.16)$$

$$\frac{\eta^2}{2}\frac{q^{n+1} - q^n}{\delta t} = \left(\frac{3}{2}\phi^n - \frac{1}{2}\phi^{n-1}\right)\frac{\phi^{n+1} - \phi^n}{\delta t}, \qquad (1.17)$$

$$\frac{\tilde{u}^{n+1} - u^n}{\delta t} - \nu\Delta\left(\frac{\tilde{u}^{n+1} + u^n}{2}\right) + B\left(\left(\frac{3}{2}u^n - \frac{1}{2}u^{n-1}\right), \left(\frac{\tilde{u}^{n+1} + u^n}{2}\right)\right)$$

$$+\nabla p^n + \frac{\dot{\phi}^{n+1}}{M} \cdot \nabla\left(\frac{3}{2}\phi^n - \frac{1}{2}\phi^{n-1}\right) = 0, \qquad (1.18)$$

with boundary conditions

$$\partial_n \phi^{n+1}|_{\partial\Omega} = 0, \tilde{u}^{n+1}|_{\partial\Omega} = 0, \partial_n q^{n+1}|_{\partial\Omega} = 0, \qquad (1.19)$$

where

$$B(u,v) := (u \cdot \nabla)v + \frac{1}{2}(\nabla \cdot u)v, \qquad (1.20)$$

$$\dot{\phi}^{n+1} = \frac{\phi^{n+1} - \phi^n}{\delta t} + \left(\frac{\tilde{u}^{n+1} + u^n}{2}\right) \cdot \nabla\left(\frac{3}{2}\phi^n - \frac{1}{2}\phi^{n-1}\right). \qquad (1.21)$$

Step 2:

$$\frac{u^{n+1} - \tilde{u}^{n+1}}{\delta t} + \frac{1}{2}\nabla(p^{n+1} - p^n) = 0, \qquad (1.22)$$

$$\nabla \cdot u^{n+1} = 0, \qquad (1.23)$$

$$u^{n+1} \cdot n|_{\partial\Omega} = 0. \qquad (1.24)$$

Several remarks are in order.

Remark 1.3.1. *In fact, (1.17) can be rewritten as*

$$q^{n+1} = q^n + \frac{2}{\eta^2}\bar{\phi}^{n+\frac{1}{2}}(\phi^{n+1} - \phi^n), \qquad (1.25)$$

where $\bar{\phi}^{n+\frac{1}{2}} = \frac{3}{2}\phi^n - \frac{1}{2}\phi^{n-1}$. *Thus we can replace the* q^{n+1} *in (1.16), it is equivalent to the following.*

$$\dot{\phi}^{n+1} - \lambda M(\Delta\frac{\phi^{n+1} + \phi^n}{2}) + \lambda M\bar{\phi}^{n+\frac{1}{2}}\left(\frac{1}{\eta^2}\bar{\phi}^{n+\frac{1}{2}}(\phi^{n+1} - \phi^n) + q^n\right) = 0. \qquad (1.26)$$

Therefore, we can solve for ϕ^{n+1} and $\tilde{u}^{n+1}$ directly from (1.26) and (1.18). Once we obtain ϕ^{n+1}, the q^{n+1} is automatically given in (1.25). Namely, the new variable q does not involve any extra computational costs.

Remark 1.3.2. *We note that q^{n+1} is formally a second order approximation of $\frac{\phi^2-1}{\eta^2}$. Indeed, Eq. (1.17) implies that*

$$q^{n+1} - \frac{(\phi^{n+1})^2 - 1}{\eta^2} + \frac{1}{2}\frac{(\phi^{n+1} - \phi^n)^2}{\eta^2} = q^n - \frac{(\phi^n)^2 - 1}{\eta^2} + \frac{1}{2}\frac{(\phi^n - \phi^{n-1})^2}{\eta^2} + R_{n+1} \quad (1.27)$$

where $R_{n+1} = -\frac{1}{2\eta^2}(\phi^{n+1} - 2\phi^n + \phi^{n-1})^2$. Since, heuristically, $R_k = O(\delta t^4)$ for $0 \le k \le n$ and assuming $q^1 - \frac{(\phi^1)^2-1}{\eta^2} + \frac{1}{2}\frac{(\phi^1-\phi^0)^2}{\eta^2} = O(\delta t^2)$ (for instance, by a first order approximation), we then get $q^{n+1} - \frac{(\phi^{n+1})^2-1}{\eta^2} + \frac{1}{2}\frac{(\phi^{n+1}-\phi^n)^2}{\eta^2} = O(\delta t^2)$. Notice that $(\phi^{n+1} - \phi^n)^2 \sim O(\delta t^2)$, therefore, q^{n+1} is formally a second order approximation to $\frac{\phi^2-1}{\eta^2}$.

Remark 1.3.3. *A second order pressure correction scheme [43] is used to decouple the computations of pressure from that of the velocity. This projection methods are analyzed in [66] where it is shown (discrete time, continuous space) that the schemes are second order accurate for velocity in $\ell^2(0,T;L^2(\Omega))$ but only first order accurate for pressure in $\ell^\infty(0,T;L^2(\Omega))$. The loss of accuracy for pressure is due to the artificial boundary condition (1.22) imposed on pressure [20]. We also remark that the Crank-Nicolson scheme with linear extrapolation is a popular time discretization for the Navier-Stokes equation. We refer to [39] and references therein for analysis on this type of discretization.*

Remark 1.3.4. *$B(u,v)$ is the skew-symmetric form of the nonlinear advection term in the Navier-Stokes equation, which is first introduced by Temam [72]. If the velocity is divergence free, then $B(u,u) = (u \cdot \nabla)u$. We define*

$$\mathbf{b}(u,v,w) := (B(u,v),w). \quad (1.28)$$

10

In our numerical scheme $\left(\frac{\tilde{u}^{n+1}+u^n}{2}\right)$ is not divergence free, but notice the following identity

$$\mathbf{b}(u,v,v) = (B(u,v),v) = 0, \ \ if \ u \cdot n|_{\partial\Omega} = 0. \tag{1.29}$$

In other words, this identity holds regardless of whether u or v are divergence free or not, which would help to preserve the discrete energy stability.

Remark 1.3.5. • *It is remarkable that in [70], the authors proposed some linearized schemes for Allen-Cahn equation (no flow case) using the second order backward differentiation formulas (BDF2), where the nonlinear term $f(\phi)$ is treated by second order extrapolation. However, the linear second order scheme in [70] is conditionally stable where there exists a constraint on the time step. The authors in [70] also developed a second order, unconditional stable scheme based on the Crank-Nicolson method, however, the obtained schemes are nonlinear. In [77], the authors developed a second order, linear, unconditionally stabilized scheme for Cahn-Hilliard equation (no flow case) based on the convex splitting approach for the modified functional $\tilde{F}(\phi)$ (the functional $F(\phi)$ is modified to get uniform upper bound for its second order derivative). However, a high order stabilizer term $(\Delta^2(\phi^{n+1} - \phi^n)$ for Cahn-Hilliard equation, analogously $\Delta(\phi^{n+1} - \phi^n)$ for Allen-Cahn equation) is added in their scheme that has higher splitting error $O(\delta t\|\phi_t\|_{H^2})$ from spatial derivatives, that is somewhat not resonable because the splitting error is much higher than the explicit treatment for the nonlinear term of $f(\phi^n)$.*

• *The framework of the above scheme takes the second order Crank-Nicolson to discretize the phase equation (1.16)-(1.17). Inspired from [31], we introduce a new variable $q(x)$ thus the order of Ginzburg-Landau double well potential is reduced by half. By some explicit-implicit treatments, we obtain a linear scheme (1.16)-(1.17) while maintaining the second order accuracy As we shall*

show below, the above scheme is unconditionally energy stable. It is noticable the discrete energy we obtained is the modified energy (1.31), where the nonlinear potential $F(\phi)$ is replaced by the term of q^2. We emphasize that the obtained dissipation law in (1.30) is a second order approximation of the PDE energy law (1.14) (note that the energy law is "=" in stead of "$\leq$"). To the best of the our knowledge, this is the first such unconditionally stable, second order, and linearized scheme for the hydrodynamics coupled phase field model.

Theorem 1.3.1. *The solution of (1.16)-(1.24) satisfies the following discrete energy law*

$$
E(u^{n+1}, \phi^{n+1}, q^{n+1}) + \frac{\delta t^2}{8} \|\nabla p^{n+1}\|^2
$$
$$
= E(u^n, \phi^n, q^n) + \frac{\delta t^2}{8} \|\nabla p^n\|^2 - \delta t \Big(\frac{1}{M} \|\dot{\phi}^{n+1}\|^2 + \nu \Big\| \nabla \Big(\frac{\tilde{u}^{n+1} + u^n}{2} \Big) \Big\|^2 \Big), \tag{1.30}
$$

where

$$
E(u, \phi, q) = \frac{1}{2} \|u\|^2 + \lambda \Big(\frac{1}{2} \|\nabla \phi\|^2 + \frac{\eta^2}{4} \|q\|^2 \Big), \tag{1.31}
$$

thus the scheme is unconditionally stable.

Proof. By taking the L^2 inner product of (1.16) with $\frac{\phi^{n+1} - \phi^n}{M \delta t}$, and performing integration by parts, we obtain

$$
\frac{1}{M} \|\dot{\phi}^{n+1}\|^2 - \frac{1}{M} \Big(\dot{\phi}^{n+1}, \Big(\frac{\tilde{u}^{n+1} + u^n}{2} \Big) \cdot \nabla \Big(\frac{3}{2} \phi^n - \frac{1}{2} \phi^{n-1} \Big) \Big)
$$
$$
+ \frac{\lambda}{\delta t} \Big(\frac{1}{2} \|\nabla \phi^{n+1}\|^2 - \frac{1}{2} \|\nabla \phi^n\|^2 \Big)
$$
$$
+ \frac{\lambda}{\delta t} \Big(\Big(\frac{3}{2} \phi^n - \frac{1}{2} \phi^{n-1} \Big) \frac{q^{n+1} + q^n}{2}, \phi^{n+1} - \phi^n \Big) \tag{1.32}
$$
$$
= 0.
$$

By taking the L^2 inner product of (1.17) with $\lambda \frac{q^{n+1} + q^n}{2}$, we obtain

$$
\frac{\lambda \eta^2}{4 \delta t} (\|q^{n+1}\|^2 - \|q^n\|^2) - \frac{\lambda}{\delta t} \Big(\Big(\frac{3}{2} \phi^n - \frac{1}{2} \phi^{n-1} \Big) \frac{q^{n+1} + q^n}{2}, \phi^{n+1} - \phi^n \Big) = 0. \tag{1.33}
$$

12

By taking the L^2 inner product of (1.18) with $\frac{\tilde{u}^{n+1}+u^n}{2}$, and using identity (1.29), we obtain

$$\frac{1}{2\delta t}(\|\tilde{u}^{n+1}\|^2 - \|u^n\|^2) + \nu\left\|\nabla\left(\frac{\tilde{u}^{n+1}+u^n}{2}\right)\right\|^2 + \left(\nabla p^n, \frac{\tilde{u}^{n+1}+u^n}{2}\right)$$
$$+ \frac{1}{M}\left(\dot{\phi}^{n+1}\nabla\left(\frac{3}{2}\phi^n - \frac{1}{2}\phi^{n-1}\right), \frac{\tilde{u}^{n+1}+u^n}{2}\right) \qquad (1.34)$$
$$= 0,$$

By taking the L^2 inner product of (1.22) with u^{n+1} and performing integration by parts, we have

$$\frac{1}{2\delta t}(\|u^{n+1}\|^2 - \|\tilde{u}^{n+1}\|^2 + \|u^{n+1} - \tilde{u}^{n+1}\|^2) = 0, \qquad (1.35)$$

where we use explicitly the divergence-free condition for u^{n+1},

$$\left(\nabla(p^{n+1} - p^n), u^{n+1}\right) = -\left((p^{n+1} - p^n), \nabla \cdot u^{n+1}\right) = 0.$$

We rewrite the projection step (1.22) as

$$\frac{1}{\delta t}\left(u^{n+1} + u^n - 2\left(\frac{\tilde{u}^{n+1}+u^n}{2}\right)\right) + \frac{1}{2}\nabla(p^{n+1} - p^n) = 0.$$

By taking the inner product of the above equation with $\frac{\delta t}{2}\nabla p^n$, one arrives at

$$\frac{\delta t}{8}\left(\|\nabla p^{n+1}\|^2 - \|\nabla p^n\|^2 - \|\nabla(p^{n+1} - p^n)\|^2\right) = \left(\nabla p^n, \left(\frac{\tilde{u}^{n+1}+u^n}{2}\right)\right). \qquad (1.36)$$

On the other hand, it follows directly from (1.22) that

$$\frac{\delta t}{8}\|\nabla(p^{n+1} - p^n)\|^2 = \frac{1}{2\delta t}\|u^{n+1} - \tilde{u}^{n+1}\|^2. \qquad (1.37)$$

Hence, by combining (1.32)-(1.37), we obtain

$$\frac{1}{M}\|\dot{\phi}^{n+1}\|^2 + \frac{\lambda}{\delta t}\left(\frac{1}{2}\|\nabla\phi^{n+1}\|^2 - \frac{1}{2}\|\nabla\phi^n\|^2\right) + \frac{\lambda}{\delta t}\frac{\eta^2}{4}(\|q^{n+1}\|^2 - \|q^n\|^2)$$
$$+ \frac{1}{2\delta t}(\|u^{n+1}\|^2 - \|u^n\|^2) + \nu\left\|\nabla\left(\frac{\tilde{u}^{n+1}+u^n}{2}\right)\right\|^2$$
$$+ \frac{\delta t}{8}\left(\|\nabla p^{n+1}\|^2 - \|\nabla p^n\|^2\right) \qquad (1.38)$$
$$= 0.$$

This concludes the proof. $\qquad\qquad\qquad\qquad\qquad\qquad\qquad\qquad\qquad\qquad\qquad\square$

Remark 1.3.6. *It is obvious that $\frac{1}{\delta t}\Big(E(u^{n+1},\phi^{n+1},q^{n+1})+\frac{\delta t^2}{8}\|\nabla p^{n+1}\|^2-E(u^n,\phi^n,q^n)-$*
$\frac{\delta t^2}{8}\|\nabla p^n\|^2\Big)$ is a second order approximation of $\frac{d}{\delta t}E(u,\phi,q)$ at $t^{n+\frac{1}{2}}$.

The similar scheme can be applied to the CHNS model, the scheme reads as follows.

*S*tep 1:

$$\frac{\phi^{n+1}-\phi^n}{\delta t}+\Big(\frac{\tilde{u}^{n+1}+u^n}{2}\Big)\cdot\nabla\Big(\frac{3}{2}\phi^n-\frac{1}{2}\phi^{n-1}\Big)-M\Delta\mu^{n+\frac{1}{2}}=0, \qquad (1.39)$$

$$\mu^{n+\frac{1}{2}}=-\lambda\Big(\Delta\frac{\phi^{n+1}+\phi^n}{2}-\Big(\frac{3}{2}\phi^n-\frac{1}{2}\phi^{n-1}\Big)\frac{q^{n+1}+q^n}{2}\Big), \qquad (1.40)$$

$$\frac{\eta^2}{2}\frac{q^{n+1}-q^n}{\delta t}=\Big(\frac{3}{2}\phi^n-\frac{1}{2}\phi^{n-1}\Big)\frac{\phi^{n+1}-\phi^n}{\delta t}, \qquad (1.41)$$

$$\frac{\tilde{u}^{n+1}-u^n}{\delta t}-\nu\Delta\Big(\frac{\tilde{u}^{n+1}+u^n}{2}\Big)+B\Big(\Big(\frac{3}{2}u^n-\frac{1}{2}u^{n-1}\Big),\Big(\frac{\tilde{u}^{n+1}+u^n}{2}\Big)\Big)$$

$$+\nabla p^n+\mu^{n+1/2}\cdot\nabla\Big(\frac{3}{2}\phi^n-\frac{1}{2}\phi^{n-1}\Big)=0, \qquad (1.42)$$

$$\partial_n\phi^{n+1}|_{\partial\Omega}=0,\quad \partial_n\mu^{n+1/2}|_{\partial\Omega}=0,\quad \tilde{u}^{n+1}|_{\partial\Omega}=0. \qquad (1.43)$$

*S*tep 2:

$$\frac{u^{n+1}-\tilde{u}^{n+1}}{\delta t}+\frac{1}{2}\nabla(p^{n+1}-p^n)=0, \qquad (1.44)$$

$$\nabla\cdot u^{n+1}=0, \qquad (1.45)$$

$$u^{n+1}\cdot n|_{\partial\Omega}=0. \qquad (1.46)$$

Similary, we obtain the energy stability as follows. The detailed proof is left to the interested readers.

Theorem 1.3.2. *The solution of* (1.39)-(1.46) *satisfies the following discrete energy law*

$$E(u^{n+1},\phi^{n+1},q^{n+1})+\frac{\delta t^2}{8}\|\nabla p^{n+1}\|^2$$

$$=E(u^n,\phi^n,q^n)+\frac{\delta t^2}{8}\|\nabla p^n\|^2-M\delta t\|\nabla\mu^{n+\frac{1}{2}}\|^2-\delta t\nu\Big\|\nabla\Big(\frac{\tilde{u}^{n+1}+u^n}{2}\Big)\Big\|^2.$$

where $E(u,\phi,q)=\frac{1}{2}\|u\|^2+\lambda\Big(\frac{1}{2}\|\nabla\phi\|^2+\frac{\eta^2}{4}\|q\|^2\Big)$, thus the scheme is unconditionally stable.

14

1.3.2 THE NONLINEAR SCHEME.

We now propose a second order, semi-discrete numerical scheme to solve the ACNS system based on the convex-splitting approach for the nonlinear potential $F(\phi)$. A similar scheme for solving the CHNS system had been proposed in [32].

For the nonlinear potential, we can rewrite $F(\phi)$ as the sum of a convex function and a concave function as

$$F(\phi) = F_v(\phi) + F_c(\phi) := \frac{1}{4\eta^2}\phi^4 + \frac{1}{4\eta^2}(-2\phi^2 + 1),$$

and accordingly $f(\phi) = F_v'(\phi) + F_c'(\phi)$. The idea of convex-splitting is to use explicit discretization for the concave part (i.e. $F_c'(\frac{3}{2}\phi^n - \frac{1}{2}\phi^{n-1})$) and semi-implicit discretization for the convex part. Further we approximate $F_v'(\frac{\phi^{n+1}+\phi^n}{2})$ by the Crank-Nicolson scheme

$$F_v'(\frac{\phi^{n+1} + \phi^n}{2}) \approx \frac{F_v(\phi^{n+1}) - F_v(\phi^n)}{\phi^{n+1} - \phi^n} = \frac{1}{\eta^2}\left(\frac{(\phi^{n+1})^2 + (\phi^n)^2}{2}\right)\frac{\phi^{n+1} + \phi^n}{2}.$$

Such a second order convex-splitting scheme is originally proposed and analyzed in [35, 2] in the context of phase field crystal equation, see also [71] for applications in thin film epitaxy.

Having computed $\phi^{n-1}, q^{n-1}, u^{n-1}, p^{n-1}$ and ϕ^n, q^n, u^n, p^n for $n \geq 1$, we compute $\phi^{n+1}, q^{n+1}, \tilde{u}^{n+1}, u^{n+1}, p^{n+1}$ by the following steps.

*S*tep 1:

$$\dot{\phi}^{n+1} - \lambda M\left(\Delta\frac{\phi^{n+1} + \phi^n}{2} - f_0(\phi^{n+1}, \phi^n)\right) = 0, \tag{1.47}$$

$$\frac{\tilde{u}^{n+1} - u^n}{\delta t} - \nu\Delta\left(\frac{\tilde{u}^{n+1} + u^n}{2}\right) + B\left(\left(\frac{3}{2}u^n - \frac{1}{2}u^{n-1}\right), \left(\frac{\tilde{u}^{n+1} + u^n}{2}\right)\right)$$

$$+\nabla p^n + \frac{\dot{\phi}^{n+1}}{M} \cdot \nabla\left(\frac{3}{2}\phi^n - \frac{1}{2}\phi^{n-1}\right) = 0, \tag{1.48}$$

$$\partial_n\phi^{n+1}|_{\partial\Omega} = 0, \tilde{u}^{n+1}|_{\partial\Omega} = 0. \tag{1.49}$$

where

$$\dot{\phi}^{n+1} = \frac{\phi^{n+1} - \phi^n}{\delta t} + \left(\frac{\tilde{u}^{n+1} + u^n}{2}\right) \cdot \nabla\left(\frac{3}{2}\phi^n - \frac{1}{2}\phi^{n-1}\right), \tag{1.50}$$

$$f_0(\phi^{n+1}, \phi^n) = \frac{1}{\eta^2}\left(\frac{(\phi^{n+1})^2 + (\phi^n)^2}{2}\right)\left(\frac{\phi^{n+1} + \phi^n}{2}\right) - \frac{1}{\eta^2}\left(\frac{3}{2}\phi^n - \frac{1}{2}\phi^{n-1}\right) \quad (1.51)$$

Step 2:

$$\frac{u^{n+1} - \tilde{u}^{n+1}}{\delta t} + \frac{1}{2}\nabla(p^{n+1} - p^n) = 0, \tag{1.52}$$

$$\nabla \cdot u^{n+1} = 0, \tag{1.53}$$

$$u^{n+1} \cdot n|_{\partial\Omega} = 0. \tag{1.54}$$

We show the energy stability theorem as follows.

Theorem 1.3.3. *The solution of the scheme* (1.47)-(1.54) *satisfies the discrete energy law of*

$$E(u^{n+1}, \phi^{n+1}) + \frac{\lambda}{4\eta^2}(\|\phi^{n+1} - \phi^n\|^2) + \frac{\delta t^2}{8}\|\nabla p^{n+1}\|^2$$

$$\leq E(u^n, \phi^n) + \frac{\lambda}{4\eta^2}(\|\phi^n - \phi^{n-1}\|^2) + \frac{\delta t^2}{8}\|\nabla p^n\|^2$$

$$- \delta t\left(\frac{1}{M}\|\dot{\phi}^{n+1}\|^2 + \nu\left\|\nabla\left(\frac{\tilde{u}^{n+1} + u^n}{2}\right)\right\|^2\right),$$

where $E(u, \phi) = \frac{1}{2}\|u\|^2 + \lambda\left(\frac{1}{2}\|\nabla\phi\|^2 + (F(\phi), 1)\right)$, *thus the scheme is unconditionally stable.*

Proof. The only difference between the linear scheme (1.16)-(1.24) and convex splitting scheme (1.47)-(1.54) is in the discretization of the Allen-Cahn equation.

By taking the L^2 inner product of (1.47) with $\frac{\phi^{n+1} - \phi^n}{M\delta t}$, and performing integration by parts, one obtains

$$\frac{1}{M}\|\dot{\phi}^{n+1}\|^2 - \frac{1}{M}\left(\dot{\phi}^{n+1}, \left(\frac{\tilde{u}^{n+1} + u^n}{2}\right) \cdot \nabla\left(\frac{3}{2}\phi^n - \frac{1}{2}\phi^{n-1}\right)\right)$$

$$+ \frac{\lambda}{\delta t}\left(\frac{1}{2}\|\nabla\phi^{n+1}\|^2 - \frac{1}{2}\|\nabla\phi^n\|^2\right) + \frac{\lambda}{\delta t}\left(f_0(\phi^{n+1}, \phi^n), \phi^{n+1} - \phi^n\right) = 0. \tag{1.55}$$

Recall the definition of $f_0(\phi^{n+1}, \phi^n)$ from (1.51) and the equality as follows,

$$\frac{1}{2}\left(3\phi^n - \phi^{n-1}, \phi^{n+1} - \phi^n\right)$$

$$= \frac{1}{2}\left(\phi^{n+1} + \phi^n, \phi^{n+1} - \phi^n\right) - \frac{1}{2}\left(\phi^{n+1} - 2\phi^n + \phi^{n-1}, \phi^{n+1} - \phi^n\right)$$

$$= \frac{1}{2}\left(\|\phi^{n+1}\|^2 - \|\phi^n\|^2\right) - \frac{1}{4}\left(\|\phi^{n+1} - \phi^n\|^2 - \|\phi^n - \phi^{n-1}\|^2 + \|\phi^{n+1} - 2\phi^n + \phi^{n-1}\|^2\right)$$

16

we obtain

$$\frac{1}{M}\|\dot{\phi}^{n+1}\|^2 - \frac{1}{M}\left(\dot{\phi}^{n+1},\left(\frac{\tilde{u}^{n+1}+u^n}{2}\right)\cdot\nabla\left(\frac{3}{2}\phi^n - \frac{1}{2}\phi^{n-1}\right)\right)$$

$$+ \frac{\lambda}{\delta t}\left(\frac{1}{2}\|\nabla\phi^{n+1}\|^2 - \frac{1}{2}\|\nabla\phi^n\|^2 + (F(\phi^{n+1}) - F(\phi^n),1)\right) \qquad (1.56)$$

$$+ \frac{\lambda}{\delta t}\frac{1}{4\eta^2}\left(\|\phi^{n+1}-\phi^n\|^2 - \|\phi^n - \phi^{n-1}\|^2 + \|\phi^{n+1} - 2\phi^n + \phi^{n-1}\|^2\right) = 0.$$

For the momentum equation, we get the same results as (1.34)-(1.37). Thus, by combining with (1.56), we obtain

$$\frac{1}{M}\|\dot{\phi}^{n+1}\|^2 + \frac{\lambda}{\delta t}\left(\frac{1}{2}\|\nabla\phi^{n+1}\|^2 - \frac{1}{2}\|\nabla\phi^n\|^2 + (F(\phi^{n+1}) - F(\phi^n),1)\right)$$

$$+ \frac{1}{2\delta t}(\|u^{n+1}\|^2 - \|u^n\|^2) + \nu\left\|\nabla\left(\frac{\tilde{u}^{n+1}+u^n}{2}\right)\right\|^2 + \frac{\delta t}{8}\left(\|\nabla p^{n+1}\|^2 - \|\nabla p^n\|^2\right)$$

$$+ \frac{\lambda}{\delta t}\frac{1}{4\eta^2}\left(\|\phi^{n+1}-\phi^n\|^2 - \|\phi^n - \phi^{n-1}\|^2 + \|\phi^{n+1} - 2\phi^n + \phi^{n-1}\|^2\right) \qquad (1.57)$$

$$= 0.$$

This completes the proof. $\qquad\qquad\qquad\qquad\qquad\qquad\qquad\qquad\qquad\qquad\qquad\square$

Remark 1.3.7. *Heuristically, $E(u^{n+1},\phi^{n+1}) + \frac{\lambda}{4\eta^2}\|\phi^{n+1} - \phi^n\|^2 + \frac{\delta t^2}{8}\|\nabla p^{n+1}\|^2$ is a second order approximation of $E(u^{n+1},\phi^{n+1})$, as one can write*

$$\|\phi^{n+1} - \phi^n\|^2 = \delta t^2 \|(\phi^{n+1} - \phi^n)/\delta t\|^2,$$

and $(\phi^{n+1} - \phi^n)/\delta t$ is an approximation of ϕ_t at $t^{n+1/2}$.

1.4   FULLY DISCRETE SCHEMES AND ENERGY STABILITY.

We now consider the fully discrete versions of schemes (1.16)-(1.24) and (1.47)-(1.54) to solve the system in the framework of finite element method.

Let $\mathcal{T}_h$ be a quasi-uniform triangulation of the domain Ω of mesh size h. We introduce X_h and Y_h the finite element approximations of $H_0^1(\Omega)$ and $H^1(\Omega)$ respectively based on the triangulation $\mathcal{T}_h$. In addition, we define $M_h = Y_h \cap L_0^2(\Omega) := \{q_h \in Y_h; \int_\Omega q_h dx = 0\}$. We assume that X_h and M_h are stable approximation spaces for

the velocity and pressure in the sense that there exists a constant c such that

$$\sup_{v_h \in X_h} \frac{(\nabla \cdot v_h, q_h)}{\|v_h\|_{H^1}} \geq c\|q_h\|_{L^2}, \quad \forall q_h \in M_h.$$

It is pointed out [28] that the inf-sup condition is necessary for the stability of pressure even though one may solve the projection step as a pressure Poisson equation.

For simplicity, the following notations will be used thereafter.

$$\phi_h^{n+\frac{1}{2}} = \frac{\phi_h^{n+1} + \phi_h^n}{2}, \quad \overline{\phi}_h^{n+\frac{1}{2}} = \frac{3\phi_h^n - \phi_h^{n-1}}{2}, \tag{1.58a}$$

$$\tilde{u}_h^{n+\frac{1}{2}} = \frac{\tilde{u}_h^{n+1} + u_h^n}{2}, \quad \overline{u}_h^{n+\frac{1}{2}} = \frac{3u_h^n - u_h^{n-1}}{2}, \tag{1.58b}$$

$$f_0(\phi_h^{n+1}, \phi_h^n) = \frac{1}{\eta^2}\left(\frac{1}{2}\big((\phi_h^{n+1})^2 + (\phi_h^n)^2\big)\phi_h^{n+\frac{1}{2}} - \overline{\phi}_h^{n+\frac{1}{2}}\right). \tag{1.58c}$$

1.4.1 THE FULLY DISCRETE LINEAR SCHEME.

We now give the fully discrete formulation for the linear scheme (1.16)-(1.24). In the framework of the finite element spaces above, the scheme reads as follows.

Find $(\phi_h^{n+1}, q_h^{n+1}, \tilde{u}_h^{n+\frac{1}{2}}, p_h^{n+1}, u_h^{n+1}) \in Y_h \times Y_h \times X_h \times M_h \times X_h$ such that for all $(\psi_h, v_h, g_h) \in Y_h \times X_h \times Y_h$ there hold

Step 1:

$$\left(\frac{\phi_h^{n+1} - \phi_h^n}{\delta t}, \psi_h\right) + \left(\tilde{u}_h^{n+\frac{1}{2}} \cdot \nabla\overline{\phi}_h^{n+\frac{1}{2}}, \psi_h\right) + \lambda M\left(\nabla\phi_h^{n+\frac{1}{2}}, \nabla\psi_h\right)$$

$$+ \lambda M\left(\overline{\phi}_h^{n+\frac{1}{2}}\left(\frac{1}{\eta^2}\overline{\phi}_h^{n+\frac{1}{2}}(\phi_h^{n+1} - \phi_h^n) + q_h^n\right), \psi_h\right) \tag{1.59}$$

$$= 0,$$

$$\left(\frac{2\tilde{u}_h^{n+\frac{1}{2}} - 2u_h^n}{\delta t}, v_h\right) + \nu\left(\nabla\tilde{u}_h^{n+\frac{1}{2}}, \nabla v_h\right) + \mathbf{b}\left(\overline{u}_h^{n+\frac{1}{2}}, \tilde{u}_h^{n+\frac{1}{2}}, v_h\right)$$

$$= -\left(\nabla p_h^n, v_h\right) - \frac{1}{M}\left(\left(\frac{\phi_h^{n+1} - \phi_h^n}{\delta t} + \tilde{u}_h^{n+\frac{1}{2}} \cdot \nabla\overline{\phi}_h^{n+\frac{1}{2}}\right)\nabla\overline{\phi}_h^{n+\frac{1}{2}}, v_h\right). \tag{1.60}$$

Step 2:

$$\left(\frac{u_h^{n+1} - \tilde{u}_h^{n+1}}{\delta t}, v_h\right) + \frac{1}{2}\left(\nabla(p_h^{n+1} - p_h^n), v_h\right) = 0, \tag{1.61}$$

$$\left(\nabla \cdot u_h^{n+1}, g_h\right) = 0. \tag{1.62}$$

*S*tep 3:

$$\frac{\eta^2}{2}\left(\frac{q_h^{n+1} - q_h^n}{\delta t}, \psi_h\right) = \left(\bar{\phi}_h^{n+\frac{1}{2}}\frac{\phi_h^{n+1} - \phi_h^n}{\delta t}, \psi_h\right). \tag{1.63}$$

Remark 1.4.1. *Note that the update of q_h^{n+1} in (1.63) is decoupled from the rest of equations.*

Remark 1.4.2. *We remark that the velocity u_h^{n+1} is sought in the space $X_h \subset H_0^1(\Omega)$. It implies that u_h^{n+1} satisfies the essential boundary condition $u_h^{n+1} = 0$ on $\partial\Omega_h$, whereas $u^{n+1} \in H$ satisfies $u^{n+1} \cdot n = 0$ on $\partial\Omega_h$. Here $H := \{v \in L^2(\Omega), \nabla \cdot v = 0, u^{n+1} \cdot n|_{\partial\Omega} = 0\}$. As is pointed out in [29] (Remark 3.3), X_h is a discrete approximation of H since H_0^1 is dense in H. Thus (1.61) and (1.62) can be viewed as an approximation of the Darcy problem. This formulation is shown in [29] to yield an optimal condition number for the pressure operator associated with the finite element spatial discretization.*

In order to establish the stability of the fully discrete scheme (1.59)–(1.63), for convenience, we introduce the discrete (negative) divergence operator $B_h : X_h(\subset H_0^1) \rightarrow M_h$ ($\subset H^1$, endowed with L^2 norm) such that for $u_h \in X_h$ and $q_h \in M_h$

$$(B_h u_h, q_h) := -(\nabla \cdot u_h, q_h) = (u_h, \nabla q_h) := (u_h, B_h^T q_h), \tag{1.64}$$

where $B_h^T : M_h \rightarrow X_h$ is the transpose of B_h (the discrete gradient operator). Thus one can write the projection step (1.61) and (1.62) in the discrete form

$$u_h^{n+1} - \tilde{u}_h^{n+1} + \frac{\delta t}{2}B_h^T(p_h^{n+1} - p_h^n) = 0, \text{ in } X_h, \tag{1.65}$$

$$B_h u_h^{n+1} = 0, \text{ in } M_h. \tag{1.66}$$

Now one can proceed by testing the above equation with $u_h^{n+1}, B_h^T p_h^{n+1} \in X_h$, respectively. The modified energy law is valid with the discrete gradient operator associated with pressure terms.

Theorem 1.4.1. *Given that $q_h^n \in Y_h$, $\phi_h^n, \phi_h^{n-1} \in Y_h$, $u_h^n, u_h^{n-1} \in X_h$, and $p_h^n \in M_h$, the system* (1.59)-(1.63) *admits a unique solution* $(\phi_h^{n+1}, q_h^{n+1}, \tilde{u}_h^{n+\frac{1}{2}}, p_h^{n+1}, u_h^{n+1}) \in Y_h \times Y_h \times X_h \times M_h \times X_h$ *at the time step t^{n+1} for any $h > 0$ and $\delta t > 0$. Moreover, the solution satisfies a discrete energy law*

$$\left(E(u_h^{n+1}, \phi_h^{n+1}, q_h^{n+1}) + \frac{\delta t^2}{8} \|B_h^T p_h^{n+1}\|^2 \right) - \left(E(u_h^n, \phi_h^n, q_h^n) + \frac{\delta t^2}{8} \|B_h^T p_h^n\|^2 \right)$$

$$\leq -\delta t \nu \|\nabla \tilde{u}_h^{n+\frac{1}{2}}\|^2 - \frac{\delta t}{M} \left\| \frac{\phi_h^{n+1} - \phi_h^n}{\delta t} + \tilde{u}_h^{n+\frac{1}{2}} \cdot \nabla \overline{\phi}_h^{n+\frac{1}{2}} \right\|^2, \qquad (1.67)$$

where $E(u_h^n, \phi_h^n, q_h^n) = \frac{1}{2}\|u_h^n\|^2 + \lambda\left(\frac{1}{2}\|\nabla\phi_h^n\|^2 + \frac{\eta^2}{4}\|q_h^n\|^2\right)$. Thus the scheme is unconditionally stable.

Proof. We note that the scheme (1.59)–(1.63) is a linear system. Thus the unique solvability would follow from the energy law (1.67).

To establish the energy law, we define an intermediate variable $\tilde{q}_h^{n+1}$ such that

$$\tilde{q}_h^{n+1} = \frac{2}{\eta^2} \overline{\phi}_h^{n+\frac{1}{2}} (\phi_h^{n+1} - \phi_h^n) + q_h^n.$$

Then (1.59) and (1.63) can be written as

$$\left(\frac{\phi_h^{n+1} - \phi_h^n}{\delta t}, \psi_h \right) + \left(\tilde{u}_h^{n+\frac{1}{2}} \cdot \nabla \overline{\phi}_h^{n+\frac{1}{2}}, \psi_h \right)$$

$$+ \lambda M \left(\nabla \phi_h^{n+\frac{1}{2}}, \nabla \psi_h \right) + \lambda M \left(\overline{\phi}_h^{n+\frac{1}{2}} \frac{\tilde{q}_h^{n+1} + q_h^n}{2}, \psi_h \right) = 0, \quad (1.68)$$

$$\frac{\eta^2}{2} \left(\frac{\tilde{q}_h^{n+1} - q_h^n}{\delta t}, \psi_h \right) = \left(\overline{\phi}_h^{n+\frac{1}{2}} \frac{\phi_h^{n+1} - \phi_h^n}{\delta t}, \psi_h \right), \qquad (1.69)$$

$$(q_h^{n+1}, \psi_h) = (\tilde{q}_h^{n+1}, \psi_h). \qquad (1.70)$$

One can obtain the following version of energy law, by working with (1.68), (1.60), (1.61), (1.62), (1.65), (1.66), and (1.69), and by following the same proof of Theorem 1.3.1,

$$\left(E(u_h^{n+1}, \phi_h^{n+1}, \tilde{q}_h^{n+1}) + \frac{\delta t^2}{8} \|B_h^T p_h^{n+1}\|^2 \right) - \left(E(u_h^n, \phi_h^n, q_h^n) + \frac{\delta t^2}{8} \|B_h^T p_h^n\|^2 \right)$$

$$= -\nu \delta t \|\nabla \tilde{u}_h^{n+\frac{1}{2}}\|^2 - \frac{\delta t}{M} \|\frac{\phi_h^{n+1} - \phi_h^n}{\delta t} + \tilde{u}_h^{n+\frac{1}{2}} \cdot \nabla \overline{\phi}_h^{n+\frac{1}{2}}\|^2. \qquad (1.71)$$

Here $E(u_h^n, \phi_h^n, q_h^n) = \frac{1}{2}\|u_h^n\|^2 + \lambda\left(\frac{1}{2}\|\nabla\phi_h^n\|^2 + \frac{\eta^2}{4}\|q_h^n\|^2\right)$. The energy law (1.67) then follows from the fact $\|q_h^{n+1}\|Ł^2 \leq \|\tilde{q}_h^{n+1}\|Ł^2$ as is evident from (1.70). The proof of the theorem is complete.

$\square$

For completeness, we also gives the corresponding linear scheme for solving the CHNS system:

Find $(\phi_h^{n+1}, q_h^{n+1}, \mu_h^{n+\frac{1}{2}}, \tilde{u}_h^{n+\frac{1}{2}}, p_h^{n+1}, u_h^{n+1}) \in Y_h \times Y_h \times Y_h \times X_h \times M_h \times X_h$ such that for all $(\psi_h, \varphi_h, v_h, g_h) \in Y_h \times Y_h \times X_h \times Y_h$ there holds

*S*tep 1:

$$\left(\frac{\phi_h^{n+1} - \phi_h^n}{\delta t}, \psi_h\right) + \left(M\nabla\mu_h^{n+\frac{1}{2}}, \nabla\psi_h\right) - \left(\overline{\phi}_h^{n+\frac{1}{2}}\tilde{u}_h^{n+\frac{1}{2}}, \nabla\psi_h\right) = 0, \tag{1.72}$$

$$\left(\mu_h^{n+\frac{1}{2}}, \varphi_h\right) = \lambda\left(\nabla(\phi_h^{n+1/2}, \nabla\varphi_h\right) + \lambda\left(\overline{\phi}_h^{n+\frac{1}{2}}\left(\frac{1}{\eta^2}\overline{\phi}_h^{n+\frac{1}{2}}(\phi_h^{n+1} - \phi_h^n) + q_h^n\right), \varphi_h\right), \tag{1.73}$$

$$\left(\frac{2\tilde{u}_h^{n+\frac{1}{2}} - 2u_h^n}{\delta t}, v_h\right) + \left(\nu\nabla\tilde{u}_h^{n+\frac{1}{2}}, \nabla v_h\right) + \mathbf{b}\left(\overline{u}_h^{n+\frac{1}{2}}, \tilde{u}_h^{n+\frac{1}{2}}, v_h\right) = -\left(\nabla p_h^n, v_h\right) \tag{1.74}$$
$$- \lambda\left(\overline{\phi}_h^{n+\frac{1}{2}}\nabla\mu_h^{n+\frac{1}{2}}, v_h\right).$$

*S*tep 2:

$$\left(\frac{u_h^{n+1} - \tilde{u}_h^{n+1}}{\delta t}, v_h\right) + \frac{\delta t}{2}\left(\nabla(p_h^{n+1} - p_h^n), v_h\right) = 0, \tag{1.75}$$

$$\left(\nabla \cdot u_h^{n+1}, g_h\right) = 0. \tag{1.76}$$

*S*tep 3:

$$\frac{\eta^2}{2}\left(\frac{q_h^{n+1} - q_h^n}{\delta t}, \psi_h\right) = \left(\overline{\phi}_h^{n+\frac{1}{2}}\frac{\phi_h^{n+1} - \phi_h^n}{\delta t}, \psi_h\right). \tag{1.77}$$

For the scheme (1.72)–(1.77), one can prove

Theorem 1.4.2. *Given that $q_h^n, \phi_h^n, \phi_h^{n-1} \in Y_h$, $u_h^n, u_h^{n-1} \in X_h$, and $p_h^n \in M_h$, the system (1.72)-(1.77) is uniquely solvable, for any $h > 0$ and $\delta t > 0$. Moreover, the solution satisfies a discrete energy law*

$$\left(E(u_h^{n+1}, \phi_h^{n+1}, q_h^{n+1}) + \frac{\delta t^2}{8}\|B_h^T p_h^{n+1}\|^2\right) - \left(E(u_h^n, \phi_h^n, q_h^n) + \frac{\delta t^2}{8}\|B_h^T p_h^n\|^2\right)$$

$$\leq -\delta t M \|\nabla \mu_h^{n+\frac{1}{2}}\|^2 - \delta t \nu \|\nabla \widetilde{u}_h^{n+\frac{1}{2}}\|^2,$$

where $E(u_h^n, \phi_h^n, q_h^n) = \frac{1}{2}\|u_h^n\|^2 + \lambda\left(\frac{1}{2}\|\nabla\phi_h^n\|^2 + \frac{\eta^2}{4}\|q_h^n\|^2\right)$. *Thus the scheme is unconditionally stable.*

Remark 1.4.3. *We point out that the modified energy stability in Theorem 1.4.1 implies the (discrete) L^2 stability for u_h^{n+1}, $\nabla\phi_h^{n+1}$ and q_h^{n+1} in the scheme (1.59)-(1.63) for the ACNS model. The H^1 stability for ϕ_h^{n+1} is not yet available, although such an estimate is valid for the original PDE as is implied by the continuous energy law Eq. (1.10). We note that formally q_h^{n+1} is a second order in-time approximation of $\frac{\phi^2-1}{\eta^2}$, as is explained in Remark 1.3.2.*

This is in contrast to the case of CHNS model. We note that the scheme (1.72)–(1.77) is mass-conservative, in the sense that $\int_\Omega \phi_h^{n+1} dx = \int_\Omega \phi_h^n dx = \cdots = \int_\Omega \phi_h^0 dx$. Hence the L^2 stability of $\nabla\phi_h^{n+1}$ in the scheme (1.72)–(1.77) plus Poincare inequality implies the H^1 stability of ϕ_h^{n+1}. These remarks are also true for the semi-discrete linear schemes (1.16)-(1.24) (ACNS) and (1.39)-(1.45) (CHNS). Note that the H^1 stability of ϕ_h^{n+1} are valid in the nonlinear schemes for both ACNS and CHNS models, see Theorem 1.4.3 and Proposition 1.4.1 below.

Remark 1.4.4. *The error analysis of the discrete schemes (1.59)-(1.63) and (1.72)– (1.77) can be very difficult. For instance, the error analysis of Eq. (1.63) would require an L^2 estimate of the derivative $\frac{\phi_h^{n+1}-\phi_h^n}{\delta t}$, which in turn needs high order estimate of ϕ_h^{n+1} via Eq. (1.59) among others. The case for CHNS could be even worse because of a lack of diffusion in q_h^{n+1} for the high order estimates of ϕ_h^{n+1}. We leave the error analysis of these schemes to a future work.*

1.4.2   THE FULLY DISCRETE NONLINEAR SCHEME.

Now we present the fully discrete version of the nonlinear scheme of (1.47)-(1.54). The scheme reads as follows.

Find $(\phi_h^{n+1}, \widetilde{u}_h^{n+\frac{1}{2}}, p_h^{n+1}, u_h^{n+1}) \in Y_h \times X_h \times M_h \times X_h$ such that for all $(\psi_h, v_h, g_h) \in Y_h \times X_h \times Y_h$, there hold,

*S*tep 1:

$$\left(\frac{\phi_h^{n+1} - \phi_h^n}{\delta t}, \psi_h\right) + \left(\widetilde{u}_h^{n+\frac{1}{2}} \cdot \nabla \overline{\phi}_h^{n+\frac{1}{2}}, \psi_h\right) + \lambda M\left(\nabla \phi_h^{n+1/2}, \nabla \psi_h\right)$$
$$+ \frac{\lambda M}{4\eta^2}\left(\left((\phi_h^{n+1})^2 + (\phi_h^n)^2\right)\left(\phi_h^{n+1} + \phi_h^n\right), \psi_h\right) = \frac{\lambda M}{\eta^2}\left(\overline{\phi}_h^{n+\frac{1}{2}}, \psi_h\right), \quad (1.78)$$

$$\left(\frac{2\widetilde{u}_h^{n+\frac{1}{2}} - 2u_h^n}{\delta t}, v_h\right) + \nu\left(\nabla \widetilde{u}_h^{n+\frac{1}{2}}, \nabla v_h\right) + \mathbf{b}\left(\overline{u}_h^{n+\frac{1}{2}}, \widetilde{u}_h^{n+\frac{1}{2}}, v_h\right)$$
$$= -\left(\nabla p_h^n, v_h\right) - \frac{1}{M}\left(\left(\frac{\phi_h^{n+1} - \phi_h^n}{\delta t} + \widetilde{u}_h^{n+\frac{1}{2}} \cdot \nabla \overline{\phi}_h^{n+\frac{1}{2}}\right)\nabla \overline{\phi}_h^{n+\frac{1}{2}}, v_h\right). \quad (1.79)$$

*S*tep 2:

$$\left(\frac{u_h^{n+1} - \widetilde{u}_h^{n+1}}{\delta t}, v_h\right) + \frac{1}{2}\left(\nabla(p_h^{n+1} - p_h^n), v_h\right) = 0, \tag{1.80}$$

$$\left(\nabla \cdot u_h^{n+1}, g_h\right) = 0. \tag{1.81}$$

The following theorem states that the fully discrete scheme (1.78)–(1.81) is unconditionally uniquely solvable and satisfies a discrete energy law.

Theorem 1.4.3. *Given that $\phi_h^n, \phi_h^{n-1} \in Y_h$, $u_h^n, u_h^{n-1} \in X_h$, and $p_h^n \in M_h$, the system (1.78)-(1.81) admits a unique solution $(\phi_h^{n+1}, \widetilde{u}_h^{n+\frac{1}{2}}, p_h^{n+1}, u_h^{n+1}) \in Y_h \times X_h \times M_h \times X_h$ at the time step t^{n+1} for any parameters $h > 0$ and $\delta t > 0$. Moreover, the solution satisfies a discrete energy law*

$$\left(E(u_h^{n+1}, \phi_h^{n+1}) + \frac{\lambda}{4\eta^2}\|\phi_h^{n+1} - \phi_h^n\|^2 + \frac{\delta t^2}{8}\|B_h^T p_h^{n+1}\|^2\right)$$
$$- \left(E(u_h^n, \phi_h^n) + \frac{\lambda}{4\eta^2}\|\phi_h^n - \phi_h^{n-1}\|^2 + \frac{\delta t^2}{8}\|B_h^T p_h^n\|^2\right)$$
$$\leq -\delta t\nu\|\nabla \widetilde{u}_h^{n+\frac{1}{2}}\|^2 - \frac{\delta t}{M}\left\|\frac{\phi_h^{n+1} - \phi_h^n}{\delta t} + \widetilde{u}_h^{n+\frac{1}{2}} \cdot \nabla \overline{\phi}_h^{n+\frac{1}{2}}\right\|^2,$$

where $E(u_h^n, \phi_h^n) = \frac{1}{2}\|u_h^n\|^2 + \lambda\left(\frac{1}{2}\|\nabla \phi_h^n\|^2 + (F(\phi_h^n), 1)\right)$. Thus the scheme is unconditionally stable.

Proof. Note that (1.80) and (1.81) (or equivalent (1.65) and (1.66)) are decoupled from the rest of the system. Given $\tilde{u}_h^{n+1}$ (or equivalent $\tilde{u}_h^{n+\frac{1}{2}}$), the unique solvability of (1.80) and (1.81) is classical, see for instance [29]. Hence one only needs to show that (1.78) and (1.79) are uniquely solvable. We define a finite dimensional Hilbert space $\mathbf{Z}_h := Y_h \times X_h$ endowed with the usual H^1 inner product and norm. We introduce an operator $S_h : \mathbf{Z}_h \to \mathbf{Z}_h$ such that

$$
\begin{aligned}
\Big(S_h(\phi_h, u_h), (\psi_h, v_h)\Big)_{\mathbf{Z}_h} &= \frac{1}{M}\Big(\frac{\phi_h - \phi_h^n}{\delta t} + u_h \cdot \nabla \overline{\phi}_h^{n+\frac{1}{2}}, \frac{\psi_h}{\delta t}\Big) + \frac{\lambda}{2}\Big(\nabla(\phi_h + \phi_h^n), \nabla \frac{\psi_h}{\delta t}\Big) \\
&\quad + \frac{\lambda}{4\eta^2}\Big(\big((\phi_h)^2 + (\phi_h^n)^2\big)(\phi_h + \phi_h^n), \frac{\psi_h}{\delta t}\Big) - \frac{\lambda}{\eta^2}\Big(\overline{\phi}_h^{n+\frac{1}{2}}, \frac{\psi_h}{\delta t}\Big) \\
&\quad + \Big(\frac{2u_h - 2u_h^n}{\delta t}, v_h\Big) + \nu\big(\nabla u_h, \nabla v_h\big) + \mathbf{b}\big(\overline{u}_h^{n+\frac{1}{2}}, u_h, v_h\big) \\
&\quad + \big(\nabla p_h^n, v_h\big) + \frac{1}{M}\Big(\big(\frac{\phi_h - \phi_h^n}{\delta t} + u_h \cdot \nabla \overline{\phi}_h^{n+\frac{1}{2}}\big)\nabla \overline{\phi}_h^{n+\frac{1}{2}}, v_h\Big),
\end{aligned}
$$

for $(\phi_h, u_h) \in \mathbf{Z}_h$ and $(\psi_h, v_h) \in \mathbf{Z}_h$. Note that Eq. (1.78) is scaled by $\frac{1}{M\delta t}$ in the definition of S_h. It is clear from Sobolev embedding and Hölder's inequality that the operator S_h is a continuous operator. We proceed to show that $\Big(S_h(\phi_h, u_h), (\phi_h, u_h)\Big)_{\mathbf{Z}_h} > 0$, for $\|(\phi_h, u_h)\|_{\mathbf{Z}_h}$ large enough. Then Lemma 1.4 in [73] (pp. 164) implies that there exists $(\phi_h^{n+1}, \tilde{u}_h^{n+\frac{1}{2}}) \in \mathbf{Z}_h$ such that $S_h(\phi_h^{n+1}, \tilde{u}_h^{n+\frac{1}{2}}) = 0$.

We have

$$
\begin{aligned}
&\frac{1}{M}\Big(\frac{\phi_h - \phi_h^n}{\delta t} + u_h \cdot \nabla \overline{\phi}_h^{n+\frac{1}{2}}, \frac{\phi_h}{\delta t}\Big) + \frac{1}{M}\Big(\big(\frac{\phi_h - \phi_h^n}{\delta t} + u_h \cdot \nabla \overline{\phi}_h^{n+\frac{1}{2}}\big)\nabla \overline{\phi}_h^{n+\frac{1}{2}}, u_h\Big) \\
&= \frac{1}{M}\Big\|\frac{\phi_h - \phi_h^n}{\delta t} + u_h \cdot \nabla \overline{\phi}_h^{n+\frac{1}{2}}\Big\|^2 + \frac{1}{M}\Big(\frac{\phi_h - \phi_h^n}{\delta t} + u_h \cdot \nabla \overline{\phi}_h^{n+\frac{1}{2}}, \frac{\phi_h^n}{\delta t}\Big) \\
&\geq \frac{1}{M}\Big\|\frac{\phi_h - \phi_h^n}{\delta t} + u_h \cdot \nabla \overline{\phi}_h^{n+\frac{1}{2}}\Big\|^2 + \frac{1}{2M}\Big(\Big\|\frac{\phi_h}{\delta t}\Big\|^2 - \Big\|\frac{\phi_h^n}{\delta t}\Big\|^2 + \Big\|\frac{\phi_h}{\delta t} - \frac{\phi_h^n}{\delta t}\Big\|^2\Big) \\
&\quad - \frac{1}{M}\|u_h\|_{L^4}\Big\|\nabla \overline{\phi}_h^{n+\frac{1}{2}}\Big\|\Big\|\frac{\phi_h^n}{\delta t}\Big\|_{L^4} \\
&\geq \frac{1}{M}\Big\|\frac{\phi_h - \phi_h^n}{\delta t} + u_h \cdot \nabla \overline{\phi}_h^{n+\frac{1}{2}}\Big\|^2 + \frac{1}{2M}\Big(\Big\|\frac{\phi_h}{\delta t}\Big\|^2 - \Big\|\frac{\phi_h^n}{\delta t}\Big\|^2 + \Big\|\frac{\phi_h}{\delta t} - \frac{\phi_h^n}{\delta t}\Big\|^2\Big) \\
&\quad - \frac{\nu}{2}\|\nabla u_h\|^2 - C(\nu, \lambda, M, \delta t)\|\nabla \overline{\phi}_h^{n+\frac{1}{2}}\|^2\|\phi_h^n\|_{H^1}^2,
\end{aligned}
$$

where one has utilized the Sobolev embedding and the Poincaré inequality. Further-

more, applying the Young's inequality and Sobolev embedding, we can obtain

$$\frac{\lambda}{4\eta^2}\left(\left((\phi_h)^2 + (\phi_h^n)^2\right)(\phi_h + \phi_h^n), \frac{\phi_h}{\delta t}\right)$$

$$= \frac{\lambda}{4\delta t\eta^2}\int_\Omega \phi_h^4 - (\phi_h^n)^4\, dx + \frac{\lambda}{4\delta t\eta^2}\left(\left((\phi_h)^2 + (\phi_h^n)^2\right)(\phi_h + \phi_h^n), \phi_h^n\right)$$

$$\geq \frac{\lambda}{8\delta t\eta^2}\int_\Omega \phi_h^4\, dx - C(\eta, \lambda, \delta t)\|\phi_h^n\|_{H^1}^4.$$

Combing the above inequalities, and in view of the skew symmetry (1.29) of the trilinear form $\mathbf{b}(u, v, w)$, we obtain

$$\left(S_h(\phi_h, u_h), (\phi_h, u_h)\right)_{\mathbf{Z}_h} \geq C(\|\phi_h\|_{H^1}^2 + \|u_h\|_{H^1}^2)$$

$$- C(\nu, \lambda, M, \delta t)(\|\nabla p_h^n\|^2 + \|\phi_h^n\|_{H^1}^4 + \|u_h^n\| + \|\nabla \overline{\phi}_h^{n+\frac{1}{2}}\|). \tag{1.82}$$

Thus for $\|(\phi_h, u_h)\|_{\mathbf{Z}_h}$ large enough, one has $\left(S_h(\phi_h, u_h), (\phi_h, u_h)\right)_{\mathbf{Z}_h} > 0$. The existence of $(\phi_h^{n+1}, \tilde{u}_h^{n+\frac{1}{2}}) \in Y_h \times X_h$ to (1.78) and (1.79) are hence proved.

For uniqueness, suppose $(\phi_{h,(i)}^{n+1}, \tilde{u}_{h,(i)}^{n+\frac{1}{2}}), i = 1, 2$ are two solutions of (1.78) and (1.79). Then their differences $\phi_h = \phi_{h,(1)}^{n+1} - \phi_{h,(2)}^{n+1}$ and $\tilde{u}_h = \tilde{u}_{h,(1)}^{n+\frac{1}{2}} - \tilde{u}_{h,(2)}^{n+\frac{1}{2}}$ satisfy

$$\left(\frac{\phi_h}{\delta t}, \psi_h\right) + \left(\tilde{u}_h \cdot \nabla \overline{\phi}_h^{n+\frac{1}{2}}, \psi_h\right) + \frac{M\lambda}{2}\left(\nabla \phi_h, \nabla \psi_h\right)$$

$$+ \frac{M\lambda}{8\eta^2}\left(\phi_h\left((\phi_{h,(1)}^{n+1} + \phi_{h,(2)}^{n+1})^2 + (\phi_h^n + \phi_{h,(1)}^{n+1})^2 + (\phi_{h,(2)}^{n+1} + \phi_h^n)^2\right), v_h\right) \tag{1.83}$$

$$= 0, \tag{1.84}$$

and

$$\left(\frac{2\tilde{u}_h}{\delta t}, v_h\right) + \nu\left(\nabla \tilde{u}_h, \nabla v_h\right) + \mathbf{b}\left(\overline{u}_h^{n+\frac{1}{2}}, \tilde{u}_h, v_h\right) \tag{1.85}$$

$$+ \frac{1}{M}\left(\left(\frac{\phi_h}{\delta t} + \tilde{u}_h \cdot \nabla \overline{\phi}_h^{n+\frac{1}{2}}\right)\nabla \overline{\phi}_h^{n+\frac{1}{2}}, v_h\right) \tag{1.86}$$

$$= 0. \tag{1.87}$$

The uniqueness follows simply by taking the test functions $\psi_h = \frac{1}{M}\phi_h$ and $v_h = \tilde{u}_h$ in (1.84) and (1.87) respectively, and summing up the results.

Finally, for the stability of the scheme, one works with (1.78), (1.79) and abstract equations (1.65), (1.66). Following the same procedure as in the proof of Theorem 1.3.3, one derives the modified energy law (1.82). This concludes the proof.

□

We comment how to implement the nonlinear scheme (1.78)–(1.81). Note that the only nonlinear term appears in the Allen-Cahn equation (1.78). We thus adopt a Picard iteration procedure on velocity to decouple the computation of the nonlinear Allen-Cahn equation (1.78) from that of the linear Navier-Stokes equation (1.79). Denote by i the Picard iteration index. Specifically, given the velocity $\widetilde{u}^{n+\frac{1}{2},i}$, we solve for $\phi^{n+1,i+1}$ from the Allen-Cahn equation (1.78) by Newton's method. As $\phi^{n+1,i+1}$ is available, we can then proceed to solve for $\widetilde{u}^{n+\frac{1}{2},i+1}$ from the linear equations (1.79). We repeat this procedure until the relative difference between two iterations within a fixed tolerance.

Numerical simulations in [46] suggest that at least 4 grid elements across the interfacial region of thickness $\sqrt{2}\eta$ are needed for accuracy. To improve the efficiency of the algorithm, we explore the capability of adaptive mesh refinement of FreeFem++ (cf. [33]) in which a variable metric/Delaunay automatic meshing algorithm is implemented.

Finally we state without a proof that similar result as Theorem 1.4.3 also holds for the fully discrete scheme for solving CHNS system (see (4.43)–(4.47) in [32]).

Proposition 1.4.1. *Given that $\phi_h^n, \phi_h^{n-1} \in Y_h$, $u_h^n, u_h^{n-1} \in X_h$, and $p_h^n \in M_h$, there exists a unique solution $(\phi_h^{n+1}, \mu_h^{n+\frac{1}{2}}, \widetilde{u}_h^{n+\frac{1}{2}}, p_h^{n+1}, u_h^{n+1}) \in Y_h \times Y_h \times X_h \times M_h \times X_h$ to the corresponding system for solving the CHNS system for any parameters $h > 0$ and $\delta t > 0$. Moreover, the solution satisfies a discrete energy law*

$$\left(E(u_h^{n+1}, \phi_h^{n+1}) + \frac{\lambda}{4\eta^2}\|\phi_h^{n+1} - \phi_h^n\|^2 + \frac{\delta t^2}{8}\|B_h^T p^{n+1}\|^2 \right)$$

$$- \left(E(u_h^n, \phi_h^n) + \frac{\lambda}{4\eta^2}\|\phi_h^n - \phi_h^{n-1}\|^2 + \frac{\delta t^2}{8}\|B_h^T p_h^n\|^2 \right)$$

$$\leq -\delta t M \|\nabla \mu_h^{n+\frac{1}{2}}\|^2 - \delta t \nu \|\nabla \widetilde{u}_h^{n+\frac{1}{2}}\|^2.$$

Thus the scheme is unconditionally stable.

1.5 Numerical Experiments

In this section, we present some numerical results using our schemes. We use P1–P1 or P2–P2 finite element function spaces for $Y_h \times Y_h$, and P1b–P1 or Taylor-Hood (P2–P1) mixed finite element spaces for $X_h \times Y_h$. It is well-known that these approximation spaces satisfy the inf-sup conditions for the biharmonic operator and Stokes operator, respectively (cf. [14, 1]).

1.5.1 Convergence Tests.

In this subsection, we verify the second order convergence of the proposed schemes via the Cauchy convergence test. The computational domain is $[0,1] \times [0,1]$, we take uniformly 2^k grid points in each direction for k from 4 to 8 ($h = \frac{\sqrt{2}}{2^k}$), and we take a linear refinement path $\delta t = \frac{0.2}{\sqrt{2}} h$. We calculate the rate at which the Cauchy difference (e.g. $\phi_h^k - \phi_h^{k-1}$) converges to zero in the L^2 norm at the final time $T = 0.1$. Here the P1 finite element space is used for Y_h, and the mini P1b–P1 mixed finite element spaces are used for $X_h \times Y_h$. The error is expected to be at the order of $e = o(\delta t^2) + o(h^2) = o(\delta t^2)$.

For all of the convergence tests, the initial conditions are taken to be

$$\phi_0 = 0.24 \cos(2\pi x) \cos(2\pi y) + 0.4 \cos(\pi x) \cos(3\pi y),$$

$$u_0 = (-\sin(\pi x)^2 \sin(2\pi y), \sin(\pi y)^2 \sin(2\pi x)).$$

The parameters of the problem are $\eta = 0.1, M = 0.01, \lambda = 0.001, \nu = 0.1$. The errors and convergence rates are presented in Tables 1.1, 1.2, and 1.3 for the linear scheme (1.59)-(1.63) solving ACNS, the linear scheme (1.72)-(1.77) solving CHNS and nonlinear scheme (1.78)-(1.81) solving ACNS, respectively. The results show

that the schemes are of second order accuracy for ϕ and u in L^2 norm, and the rate of convergence for pressure p appear to be only first order which is known for the pressure projection scheme.

Table 1.1: Cauchy convergence test for the linear scheme (1.59)-(1.63) solving ACNS system; errors are measured in L^2 norm; 2^k grid points in each direction for k from 4 to 8, $\delta t = \frac{0.2}{2}h$, $\eta = 0.1$, $M = 0.01$, $\lambda = 0.001$, $\nu = 0.1$.

	$16-32$	rate	$32-64$	rate	$64-128$	rate	$128-256$
ϕ	$1.50e-3$	1.86	$4.21-4$	1.96	$1.08e-4$	1.99	$2.72e-5$
u	$3.00e-3$	2.04	$7.24e-4$	2.03	$1.77e-4$	2.02	$4.38e-5$
v	$3.00e-3$	2.03	$7.37e-4$	2.03	$1.81e-4$	2.02	$4.48e-5$
p	$1.65e-2$	1.44	$6.10e-3$	1.43	$2.30e-3$	1.42	$8.40e-4$

Table 1.2: Cauchy convergence test for the linear scheme (1.72)-(1.76) solving CHNS system; errors are measured in L^2 norm; 2^k grid points in each direction for k from 4 to 8, $\delta t = \frac{0.2}{2}h$, $\eta = 0.1$, $M = 0.01$, $\lambda = 0.001$, $\nu = 0.1$.

	$16-32$	rate	$32-64$	rate	$64-128$	rate	$128-256$
ϕ	$3.31e-2$	2.02	$8.10-3$	1.99	$2.01e-4$	1.98	$5.17e-4$
u	$3.00e-3$	2.04	$7.25e-4$	2.03	$1.78e-4$	2.02	$4.39e-5$
v	$3.10e-3$	2.03	$7.49e-4$	2.02	$1.84e-4$	2.01	$4.56e-5$
p	$1.65e-2$	1.44	$6.10e-3$	1.42	$2.30e-3$	1.41	$8.53e-4$

Table 1.3: Cauchy convergence test for the nonlinear convex-splitting scheme (1.78)-(1.81) solving ACNS system; errors are measured in L^2 norm; 2^k grid points in each direction for k from 4 to 8, $\delta t = \frac{0.2}{2}h$, $\eta = 0.1$, $M = 0.01$, $\lambda = 0.001$, $\nu = 0.1$.

	$16-32$	rate	$32-64$	rate	$64-128$	rate	$128-256$
ϕ	$1.60e-3$	1.86	$4.34-4$	1.96	$1.11e-4$	1.99	$2.80e-4$
u	$3.00e-3$	2.04	$7.24e-4$	2.03	$1.78e-4$	2.02	$4.38e-5$
v	$3.00e-3$	2.03	$7.36e-4$	2.03	$1.81e-4$	2.02	$4.47e-5$
p	$1.65e-2$	1.44	$6.10e-3$	1.43	$2.30e-3$	1.42	$8.40e-4$

1.5.2 THE VELOCITY OF A CIRCULAR MOVING INTERFACE.

Here we perform a classical numerical experiment of a shrinking circular bubble [13] for Allen-Cahn equation ($u = 0$, no flow). We show that we can accurately

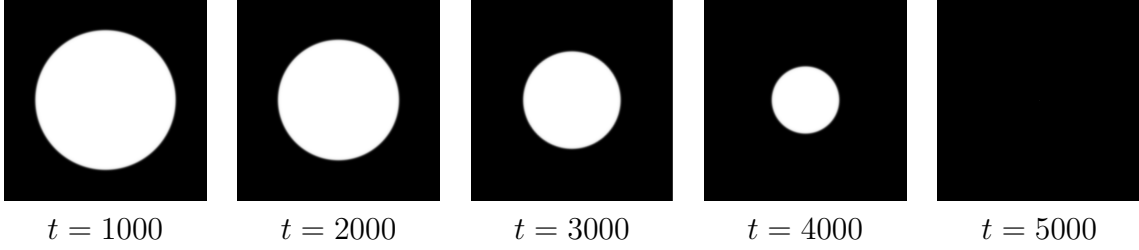$$t = 1000 \qquad t = 2000 \qquad t = 3000 \qquad t = 4000 \qquad t = 5000$$

Figure 1.1: Temporal evolution of a circular domain driven by mean curvature without hydrodynamic effects. The parameters are $\eta = 1.0$, $M = 1.0$, $\lambda = 1.0$, $\delta t = 0.1$, $\Omega = [0, 256] \times [0, 256]$.
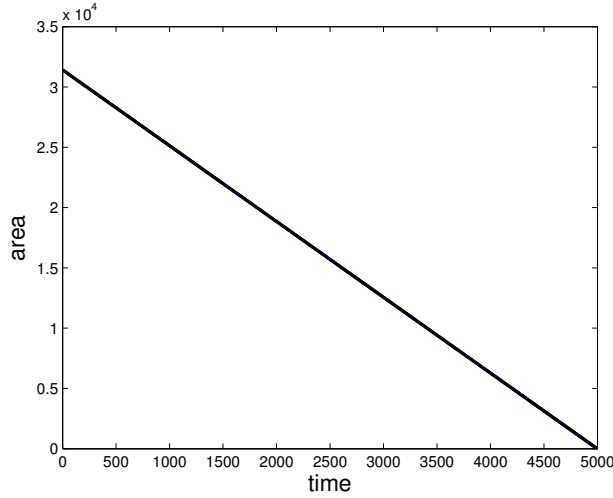

Figure 1.2: The areas of the circle as a function of time. $\eta = 1.0$, $M = 1.0$, $\lambda = 1.0$, $\delta t = 0.1$, $\Omega = [0, 256] \times [0, 256]$. The slope of the line is -6.2842 and the theoretical slope is -2π.

calculate the velocity of a moving interface via our second order schemes. The set-up of the numerical experiment is the same as of that in [13] with the domain size of $\Omega = [0, 256] \times [0, 256]$. The parameters are taken to be unity, i.e., $\eta = 1$, $M = 1$, $\lambda = 1$. Initially, there is a circular interface boundary of radius 100 in the middle of Ω. Within the circle the phase variable is $+1$ and outside it takes the value -1. As it is pointed out in [13], the circular boundary will shrink and disappear eventually driven by the mean curvature. The area of the circle can be found explicitly, $A = A_0 - 2\pi t$, where A_0 is the initial area. Thus the circular boundary shrinks at a rate of $V = 2\pi$.

The temporal evolution of the circular domain is shown in Fig. 1.1. We take

29

$\delta t = 0.1$ in the simulation. In space, we explore the adaptive mesh refinement of FreeFem++ (cf. [33]) such that at least four grid cells are located across the diffuse interface ($h_{min} \approx 0.2$). The results shown are produced using the linear scheme (1.16)-(1.24), and the same results are obtained via the nonlinear convex splitting scheme.

The areas of the circle as a function of time is shown in Fig. 1.2. The slope of the line is approximately -6.2842. The relative error of the velocity compared to the theory is $1.61e - 04$. Our scheme performs better than any of the schemes presented in [13] in this regard.

1.5.3 SHAPE RELAXATION.

In this subsection, we perform another two standard numerical tests in the context of phase field fluid models– shape relaxation in Fig. 1.3 and Fig. 1.4. In both tests, the P2 finite element space is used for Y_h, and the Taylor-Hood P2–P1 mixed finite element spaces are used for $X_h \times Y_h$.

| $t = 4$ | $t = 40$ | $t = 60$ | $t = 80$ |
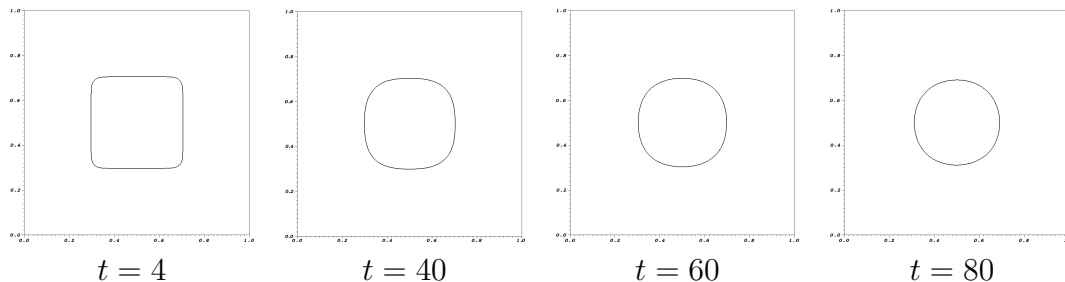
Figure 1.3: Snapshots of the relaxation of a square shape by the ACNS system. $\eta = 0.01$, $\lambda = M = 0.0001$, $\delta t = 0.05$.

In the first numerical test, we simulate the square evolves to a circular bubble using the linear scheme (1.59)-(1.63) for the ACNS system. The phase variable ϕ takes value $+1$ inside the square and -1 outside of it. The initial velocity u and pressure p are zeros. The parameters are $\eta = 0.01$, $\lambda = M = 0.0001$, $\nu = 0.1$, $\delta t = 0.05$. Fig. 1.3 shows some snapshots of the zero contour of the order parameter

of the ACNS system. We observe that the isolated square shape relaxes to a circular shape, due to the effect of surface tension. The shape also appears to shrink a bit during the relaxation because the ACNS system is not mass-conservative.

In the second numerical test, we simulate the merging process of two circular bubbles using the CHNS system. In Fig. 1.4, we show the merging of two circles next to each other under the influence of surface tension in the CHNS system. The circles quickly connect and eventually relax to a large circle at which the surface energy is minimal. In this simulation, the parameters are $\eta = 0.01$, $\lambda = 0.0001$, $M = 0.1$, $\nu = 0.1$, $\delta t = 0.01$.
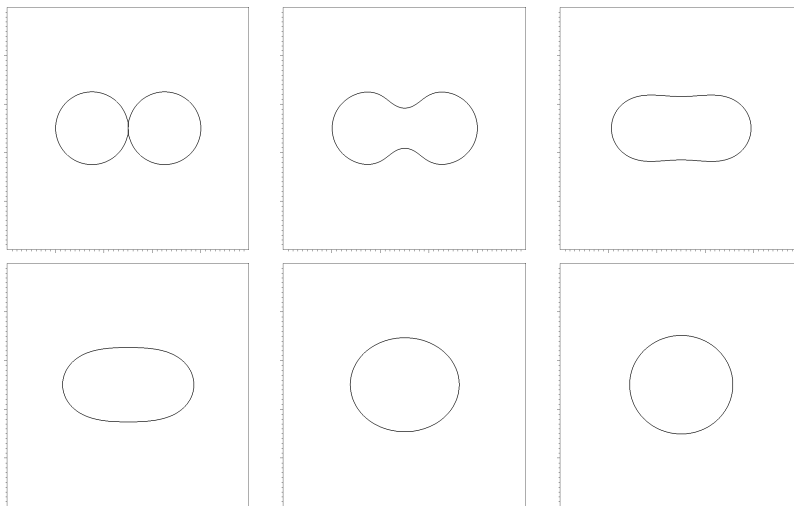
Figure 1.4: Zero contour plots of the merging and relaxation of two kissing circles by the CHNS system. From left to right, $t = 0.0$, $t = 0.2$, $t = 2$, $t = 4$, $t = 12$, $t = 18$. $\eta = 0.01$, $\lambda = 0.0001$, $M = 0.1$, $\nu = 0.1$, $\delta t = 0.01$.

1.5.4 A Rising Bubble.

In this numerical experiment, we simulate the rising process of a lighter liquid bubble using the CHNS system driven by the buoyancy. In particular, the density difference of the two fluids is small so that a Boussinesq approximation is applicable [56]. Specifically, a buoyancy term $G(\rho(\phi) - \bar{\rho})\hat{y} := B(\phi - \bar{\phi})\hat{y}$ is added to Navier-

Stokes equation. Here $\rho(\phi) = \frac{1+\phi}{2}\rho_1 + \frac{1-\phi}{2}\rho_2$, $\bar{\rho}$ and $\bar{\phi}$ are the spatial averages of ρ and ϕ, $B = G\frac{\rho_1-\rho_2}{2}$, $\hat{y} = (0,1)^T$.

The filled contour plots in gray scale of the rising bubble are shown in Fig. 1.5. We see that the bubble rises due to the buoyancy. As it rises, the bubble also elongates horizontally, especially when it is near the upper boundary.
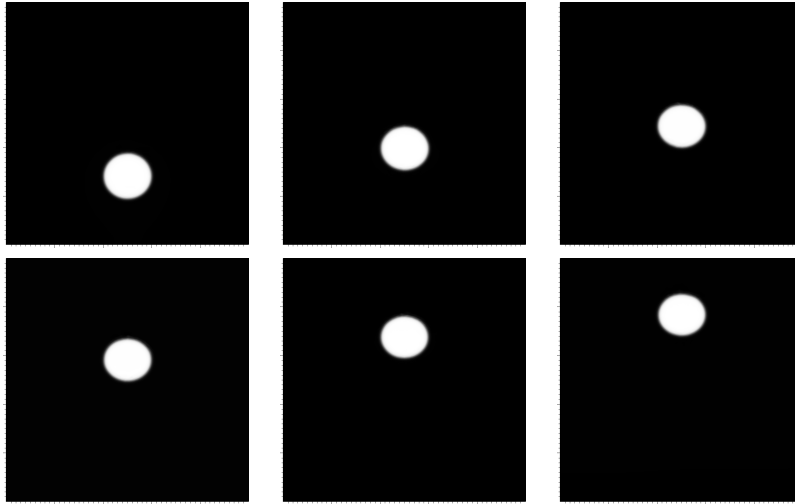

Figure 1.5: Filled contour plots in gray scale of the rising bubble by the CHNS system. From left to right, $t = 0.64$, $t = 1.2$, $t = 1.6$, $t = 2$, $t = 2.4$, $t = 2.8$. $\eta = 0.01$, $\lambda = 0.0001$, $M = 0.1$, $\nu = 0.01$, $\delta t = 0.01$, $B = 1.0$.

Chapter 2

Numerical approximations for smectic–A liquid crystal flows

2.1 Introduction

Liquid crystal (LC) is often viewed as the fourth state of the matter besides the gas, liquid and solid. It may flow like a liquid, but its molecules may be oriented in a crystal-like way. There are many different types of liquid-crystal phases, which can be distinguished by their different optical properties. Thermotropic LCs can be distinguished into two main different phases: Nematic and Smectic. In Nematic phases, the rod-shaped molecules have no positional order, but molecules self-align to have a long-range directional order with their long axes roughly parallel. Thus, the molecules are free to flow and their center of mass positions are randomly distributed as in a liquid, although they still maintain their long-range directional order. In smectic phases, which are found at lower temperatures, the well-defined layers form, that can slide over one another in a manner similar to that of soap. The smectics are thus positionally ordered along one direction inside the layer. There are many different smectic phases, all characterized by different types and degrees of positional and orientational order (cf.[11, 26]). In particular, in Smectic-A phases, molecules are oriented along the normal vector of the layers, while in Smectic-C phases they are tilted away from the normal vector of the layer.

The mathematical model of liquid crystals can often be derived from an energy-based variational formalism (energetic variational approaches), leading to well-posed

nonlinear coupled systems that satisfy thermodynamics-consistent energy dissipation laws. This makes it possible to carry out mathematical analysis and design numerical schemes which satisfy a corresponding discrete energy dissipation law. For smectic-A phase liquid crystals, in de Gennes' pioneering work [26], the phenomenonlogical free energy of smectic–A phase is presented by coupling two order parameters which represent the average direction of molecular alignment, as well as the layer structure, respectively. In [12], the authors modified the de Gennes' model by adding a second order gradient term for the smectic order parameter to investigate the nematic to smectic–A or smectic–C phase transition, and to predict the twist grain boundary phase in chiral smectic liquid crystals. In [42], the authors used the de Gennes energy to study smectic–A liquid crystals to simulate the chevron (zigzag) pattern formed in the presence of an applied magnetic field. In [19], the authors derived the hydrodynamics coupled model for smectic–A phase by assuming that the director field is strictly equal to the gradient of the layer, thus the free energy is reduced to one order parameter.

From the numerical point of view, it is specifically desired to design numerical schemes that could preserve the thermo-dynamically consistent dissipation law (energy-stable) at the discrete level, since the preservation of such laws is critical for numerical methods to capture the correct long time dynamics. The noncompliance of energy dissipation laws may lead to spurious numerical solutions if the grid and time step sizes are not carefully controlled. To the best of the author's knowledge, although a variety of the smectic liquid crystal models had been developed for more than half a centry, we notice that the successful attempts in designing efficient energy stable schemes are very scarce due to the complex nonlinearities. For instances, in [25], the authors present a temporal second order numerical scheme to solve the model of [19]. The scheme is energy stable, however, it is nonlinear thus the implementation is complicated and the computational cost might be high. In [42], the authors developed a

temporal first order scheme. However, it does not follow the energy dissipation law even though the schemes are linear and decoupled.

Therefore, the main purpose of this paper to construct the efficient schemes to solve the de Gennes type smectic–A liquid crystal model (cf. [26, 42]). We first couple the hydrodynamics to the original de Gennes free energy and derive the whole model based on the variational approach and the Ficks' law. To solve the model, the main difficulties roughly include (i) the coupling between the velocity and director field/layer function through the convection terms and nonlinear stresses; (ii) the coupling of the velocity and pressure through the incompressibility constraint; (iii) the nonlinear coupling between the director field and layer function. We develop a time discretization scheme which (a) is unconditionally stable; (b) satisfies a discrete energy law; and (c) leads to linear, decoupled equations to solve at each time step. This is by no means an easy task due to many highly nonlinear terms and the couplings existed in the model.

The rest of the chapter is organized as follows. In Section 2, we present the whole model and present the PDE energy law. In Section 3, we develop the numerical scheme and prove the unconditional stability. In Section 4, we present some numerical experiments to validate the proposed scheme. Finally, some concluding remarks are presented in Section 5.

2.2   THE SMECTIC-A LIQUID CRYSTAL FLUID FLOW MODEL AND ITS ENERGY LAW

The de Gennes free energy of smectic A liquid crystal is described by a unit vector (director field) $\boldsymbol{d}$ and a complex order parameter ψ, to represent the average direction of molecular alignment and the layer stucture, respectively. The smectic order parameter is written as

$$\psi(\boldsymbol{x}) = \rho(\boldsymbol{x})e^{iq\omega(\boldsymbol{x})}, \tag{2.1}$$

35

where $\omega(\boldsymbol{x})$ is the order parameter to describe the layer structure so that $\nabla\omega$ is perpendicular to the layer. The smectic layer density $\rho(\boldsymbol{x})$ is the mass density of the layers. The de Gennes free energy reads as follows,

$$E(\psi, \boldsymbol{d}) = \int_{\Omega} \left(C|\nabla\psi - iq\boldsymbol{d}\psi|^2 + K|\nabla\boldsymbol{d}|^2 + \frac{g}{2}(|\psi|^2 - \frac{r}{g})^2 - \chi_a \boldsymbol{\Psi}^2 (\boldsymbol{d} \cdot \boldsymbol{\mu}_1)^2 \right) d\boldsymbol{x} \quad (2.2)$$

where the order parameters C, K, g, r are all fixed positive constants, $\boldsymbol{\mu}_1$ is the unit vector representing the direction of magnetic field and $\boldsymbol{\Psi}^2$ is the strength of the applied field. $\Omega = (-L, L)^2 \times (-d, d)$.

Now we consider the simple case by assuming the density $\rho(x) = r/g$ [42], then the energy becomes

$$E(\psi, \boldsymbol{d}) = \int_{\Omega} \left(Cq^2 |\nabla\omega - \boldsymbol{d}|^2 + K|\nabla\boldsymbol{d}|^2 - \chi_a \boldsymbol{\Psi}^2 (\boldsymbol{d} \cdot \boldsymbol{\mu}_1)^2 \right) d\boldsymbol{x}. \quad (2.3)$$

Let $\phi(\boldsymbol{x}) = \frac{\omega(\boldsymbol{x})}{d}$, thus the normalized energy becomes

$$E(\phi, \boldsymbol{d}) = \lambda \int_{\tilde{\Omega}} \left(\frac{1}{\eta} \frac{|\nabla\phi - \boldsymbol{d}|^2}{2} + \eta \frac{|\nabla\boldsymbol{d}|^2}{2} - \frac{\tau}{2}(\boldsymbol{d} \cdot \boldsymbol{\mu}_1)^2 \right) d\boldsymbol{x}, \quad (2.4)$$

where

$$\tilde{\boldsymbol{x}} = \frac{\boldsymbol{x}}{d}, \ \tilde{\Omega} = (0, 2\ell)^2 \times (0, 2), \ \ell = \frac{L}{d},$$
$$\eta = \frac{\gamma}{d}, \gamma = \sqrt{\frac{K}{Cq^2}}, \ \lambda = \frac{2dK}{\eta}, \ \tau = \frac{\chi_a \boldsymbol{\Psi}^2 d^2 \eta}{K}. \quad (2.5)$$

The dimensionless parameter η is in fact the ratio of the layer thickness to the sample thickness and thus $\eta \ll 1$.

To release the unit vector constraint of $|\boldsymbol{d}| = 1$, a nonlinear potential $G(\mathbf{b}) = \frac{1}{4\epsilon^2}(|\mathbf{b}|^2 - 1)^2$ which is a Ginzburg-Landau type penalty term, is added into the free energy to approximate the unit length constraint of $\mathbf{b}$ [51, 50] , where $\epsilon \ll 1$ is a penalization parameter. Thus the modified total free energy with the hydrodynamics

$$E_{tot}(u, \phi, \boldsymbol{d}) = \int_{\tilde{\Omega}} \frac{1}{2}|u|^2 d\boldsymbol{x}$$
$$+ \lambda \int_{\tilde{\Omega}} \left(\frac{1}{\eta} \frac{|\nabla\phi - \boldsymbol{d}|^2}{2} + \eta(\frac{|\nabla\boldsymbol{d}|^2}{2} + \mathbf{G}(\boldsymbol{d})) - \frac{\tau}{2}(\boldsymbol{d} \cdot \boldsymbol{\mu}_1)^2 \right) d\boldsymbol{x}, \quad (2.6)$$

where u is the fluid velocity field.

Assuming a generalized Fick's law that the mass flux be proportional to the gradient of the chemical potential [7, 24, 54, 53], we can derive the following system:

$$\phi_t + u \cdot \nabla\phi = -M_1\mu_\phi, \ \mu_\phi = \frac{\delta E}{\delta \phi}, \tag{2.7}$$

$$\boldsymbol{d}_t + u \cdot \nabla\boldsymbol{d} = -M_2\boldsymbol{\mu}_d, \ \boldsymbol{\mu}_d = \frac{\delta E}{\delta \boldsymbol{d}}, \tag{2.8}$$

$$u_t + u \cdot \nabla u - \nabla \cdot \sigma_d + \nabla p - \mu_\phi\nabla\phi - \mu_d\nabla\boldsymbol{d} = 0, \tag{2.9}$$

$$\nabla \cdot u = 0, \tag{2.10}$$

where p is the pressure, σ_d is the Caughy stress tensor, ν is the viscosity, M_1, M_2 are the relaxation order parameters. The variational derivatives μ_ϕ and $\boldsymbol{\mu}_d$ are

$$\mu_\phi = \lambda\frac{1}{\eta}(-\Delta\phi + \nabla \cdot \boldsymbol{d}), \tag{2.11}$$

$$\boldsymbol{\mu}_d = \lambda\Big(\eta\big(-\Delta\boldsymbol{d} + \boldsymbol{g}(\boldsymbol{d})\big) + \frac{1}{\eta}(-\nabla\phi + \boldsymbol{d}) - \tau(\boldsymbol{d} \cdot \boldsymbol{\mu}_1)\boldsymbol{\mu}_1\Big), \tag{2.12}$$

where $\boldsymbol{g}(\boldsymbol{d}) = \frac{1}{\epsilon^2}\boldsymbol{d}(|\boldsymbol{d}|^2 - 1)$.

Following the work in [19], the Cauchy stress tensor σ_d reads as follows,

$$\sigma_d = \mu_1(\boldsymbol{d}^T D(u)\boldsymbol{d})\boldsymbol{d} \otimes \boldsymbol{d} + \mu_4 D(u) + \mu_5(D(u)\boldsymbol{d} \otimes \boldsymbol{d} + \boldsymbol{d} \otimes D(u)\boldsymbol{d}), \tag{2.13}$$

where $\mu_i > 0$ and $D(u) = \frac{1}{2}((\nabla u) + (\nabla u)^T)$ is the strain tensor. In this paper, we assume μ_1, μ_5 are negligible comparing to μ_4, thus the stress tensor is simplifed to

$$\sigma_d = \mu_4 D(u). \tag{2.14}$$

For simplicty, we assume the boundary conditions as follows.

$$u|_{\partial\Omega} = 0, \partial_{\boldsymbol{n}}\phi|_{\partial\Omega} = 0, \partial_{\boldsymbol{n}}\boldsymbol{d}|_{\partial\Omega} = 0, \tag{2.15}$$

where $\boldsymbol{n}$ is the outward normal of the boudary.

To obtain the dissipation law of the system (2.7)-(2.10), we take the L^2 inner product of (2.7) with $\frac{\delta E}{\delta\phi}$, (2.8) with $\frac{\delta E}{\delta\boldsymbol{d}}$, and (2.9) with u, perform the integration by

parts, and add all equalities together, we obtain

$$\frac{d}{dt}E_{tot}(u, \phi, \boldsymbol{d}) = -\int_{\Omega}\left(\mu_4|D(u)|^2 + M_1|\frac{\delta E}{\delta \phi}|^2 + M_2|\frac{\delta E}{\delta \boldsymbol{d}}|^2\right)d\boldsymbol{x}. \qquad (2.16)$$

2.3 NUMERICAL SCHEME

The emphasis of our algorithm development is placed on designing numerical schemes that are not only easy-to-implement, but also satisfy a discrete energy dissipation law. We will design schemes that in particular can overcome the following difficulties, namely,

- the coupling of the velocity and pressure through the incompressibility condition;

- the stiffness in the director equation associated with the penalty parameter η;

- the nonlinear couplings among the fluid equation, the layer equation and the director equation.

We construct an energy stable scheme based on a stabilization approach [64]. To this end, we shall assume that $\mathbf{G}(\mathbf{b})$ satisfies the following conditions, i.e.,

$$|H_{\mathbf{G}}(\boldsymbol{x})| \leq L, \forall \boldsymbol{x}. \qquad (2.17)$$

where $(H_{\mathbf{G}}(\boldsymbol{x}))_{i,j} = \frac{\partial^2 \mathbf{G}}{\partial x_i \partial x_j}, i, j = 1, 2, 3$ is the Hessian matrix of $\mathbf{G}(\boldsymbol{x})$. One immediately notes that this condition is not satisfied by this usual double-well potential. However, it is a common practice that one truncates this fourth order polynomial G to quadratic growth outside of an interval $[-M, M]$ without affecting the solution if the maximum norm of the initial condition ϕ_0 is bounded by M. Therefore, one can (cf. [45, 16, 64]) consider the truncated double-well potential $\tilde{\mathbf{G}}(\boldsymbol{d})$. We can modify

this function outside a ball in $\{\boldsymbol{x} : |\boldsymbol{d}(\boldsymbol{x})| \leq 1\} \in \mathbb{R}^3$ of radius 1 as follows.

$$\tilde{\mathbf{G}}(\boldsymbol{d}) = \begin{cases} \dfrac{1}{4\epsilon^2}(|\boldsymbol{d}|^2 - 1)^2, & |\boldsymbol{d}| \leq 1, \\ \dfrac{1}{4\epsilon^2}(|\boldsymbol{d}| - 1)^2, & |\boldsymbol{d}| > 1. \end{cases} \tag{2.18}$$

Hence, there exists a postive constant L_G such that

$$\max_{\boldsymbol{x} \in \mathbb{R}^3} |H_{\tilde{G}}(\boldsymbol{x})| \leq L_G, \tag{2.19}$$

When deriving the energy law (2.16), we notice that the nonlinear terms in $\frac{\delta \mathscr{E}_{tot}}{\delta \phi}$ and $\frac{\delta \mathscr{E}_{tot}}{\delta \boldsymbol{d}}$ involve second order derivatives, and it is not convenient to use them as test functions in numerical approximations, making it difficult to prove the discrete energy dissipation law. To overcome this difficulty, we first reformulate the system (2.7)-(2.10) in an alternative form which is convenient for numerical approximations. The system reads as follows,

$$\phi_t + u \cdot \nabla \phi = -M_1 \mu_\phi, \tag{2.20}$$

$$\boldsymbol{d}_t + u \cdot \nabla \boldsymbol{d} = -M_2 \boldsymbol{\mu}_d, \tag{2.21}$$

$$u_t + u \cdot \nabla u - \nabla \cdot \sigma_d + \nabla p + \frac{\dot{\phi}}{M_1} \nabla \phi + \frac{\dot{\boldsymbol{d}}}{M_2} \nabla \boldsymbol{d} = 0, \tag{2.22}$$

$$\nabla \cdot u = 0, \tag{2.23}$$

where $\dot{\phi} = \phi_t + u \cdot \nabla \phi$ and $\dot{\boldsymbol{d}} = \boldsymbol{d}_t + u \cdot \nabla \boldsymbol{d}$. To obtain the dissipation law of the system (2.20)-(2.23), we take the L^2 inner product of (2.20) with ϕ_t, (2.21) with $\boldsymbol{d}_t$, and (2.22) with u, perform the integration by parts, and add all equalities together. We obtain

$$\frac{d}{dt} E_{tot} = -\int_\Omega \left(\mu_4 |\nabla u|^2 + \frac{1}{M_1} |\dot{\phi}|^2 + \frac{1}{M_2} |\dot{\boldsymbol{d}}|^2 \right) d\boldsymbol{x}. \tag{2.24}$$

We now fix some notations. For scalar function u, v and vector function $\boldsymbol{u} = (u_1, u_2, u_3)$ and $\boldsymbol{v} = (v_1, v_2, v_3)$, we denote the L^2 inner product as follows.

$$(u, v) = \int_\Omega uv dx, \ \|u\|^2 = (u, u), \ (\boldsymbol{u}, \boldsymbol{v}) = \int_\Omega u \boldsymbol{v}^T d\boldsymbol{x}, \ \|\boldsymbol{u}\|^2 = (\boldsymbol{u}, \boldsymbol{u}). \tag{2.25}$$

39

Now, we are ready to present our energy stable schemes.

Our numerical scheme reads as follows. Given the initial conditions ϕ^0, ψ^0, u^0 and $p^0 = 0$, having computed ϕ^n, ψ^n, u^n and p^n for $n > 0$, we compute $\phi^{n+1}, \psi^{n+1}, \tilde{u}^{n+1}$ u^{n+1} and p^{n+1} by

Step 1:

$$
\begin{cases}
\dfrac{1}{M_1}\dot{\phi}^{n+1} = \dfrac{\lambda}{\eta}(\Delta\phi^{n+1} - \nabla \cdot \boldsymbol{d}^n), \\[2mm]
\dfrac{\partial \phi^{n+1}}{\partial \boldsymbol{n}}\Big|_{\partial\Omega} = 0,
\end{cases}
\tag{2.26}
$$

with

$$
\dot{\phi}^{n+1} = \frac{\phi^{n+1} - \phi^n}{\delta t} + (u_\star^n \cdot \nabla)\phi^n, \; u_\star^n = u^n - \delta t \frac{\dot{\phi}^{n+1}}{M_1}\nabla\phi^n.
\tag{2.27}
$$

Step 2:

$$
\begin{cases}
S(\boldsymbol{d}^{n+1} - \boldsymbol{d}^n) + \dfrac{1}{M_2}\dot{\boldsymbol{d}}^{n+1} \\[2mm]
\qquad = \lambda\Big(\eta(\Delta\boldsymbol{d}^{n+1} - \boldsymbol{g}(\boldsymbol{d}^n)) + \dfrac{1}{\eta}(\nabla\phi^{n+1} - \boldsymbol{d}^{n+1}) + \tau(\boldsymbol{d}^n \cdot \boldsymbol{\mu}_1) \cdot \boldsymbol{\mu}_1\Big), \\[2mm]
\dfrac{\partial \boldsymbol{d}^{n+1}}{\partial n}\Big|_{\partial\Omega} = 0,
\end{cases}
\tag{2.28}
$$

with

$$
\dot{\boldsymbol{d}}^{n+1} = \frac{\boldsymbol{d}^{n+1} - \boldsymbol{d}^n}{\delta t} + (u_{\star\star}^n \cdot \nabla)\boldsymbol{d}^n, \; u_{\star\star}^n = u_\star^n - \delta t \frac{\dot{\boldsymbol{d}}^{n+1}}{M_2}\nabla\boldsymbol{d}^n.
\tag{2.29}
$$

Step 3:

$$
\begin{cases}
\dfrac{\tilde{u}^{n+1} - u^n}{\delta t} + (u^n \cdot \nabla)\tilde{u}^{n+1} - \mu_4\Delta\tilde{u}^{n+1} + \nabla p^n + \dfrac{\dot{\phi}^{n+1}}{M_1}\nabla\phi^n + \dfrac{\dot{\boldsymbol{d}}^{n+1}}{M_2}\nabla\boldsymbol{d}^n = 0, \\[2mm]
\tilde{u}^{n+1}|_{\partial\Omega} = 0.
\end{cases}
\tag{2.30}
$$

Step 4:

$$
\begin{cases}
\dfrac{u^{n+1} - \tilde{u}^{n+1}}{\delta t} + \nabla(p^{n+1} - p^n) = 0, \\[2mm]
\nabla \cdot u^{n+1} = 0, \\[2mm]
\boldsymbol{n} \cdot u^{n+1}|_{\partial\Omega} = 0.
\end{cases}
\tag{2.31}
$$

In the above, S is a stabilizing parameter to be determined.

We have the following remarks in order:

- A pressure-correction scheme [27] is used to decouple the computation of the pressure from that of the velocity.

- The nonlinear term $\boldsymbol{g}(\boldsymbol{d})$ mainly takes the form like $\frac{1}{\epsilon^2}\boldsymbol{d}(|\boldsymbol{d}|^2-1)$, so the explicit treatment of this term usually leads to a severe restriction on the time step δt when $\epsilon \ll 1$. Thus we introduce in (2.26) a linear "stabilizing" term to improve the stability while preserving the simplicity. It allows us to treat the nonlinear term explicitly without suffering from any time step constraint [62, 64, 63]. Note that this stabilizing term introduces an extra consistent error of order $O(\delta t)$ in a small region near the interface, but this error is of the same order as the error introduced by treating it explicitly, so the overall truncation error is essentially of the same order with or without the stabilizing term. It is noticable that the truncation error of the stablizing approach is exactly the same as the convex splitting method [23].

- Inspired by [3, 58, 62], which deal with a phase-field model of three-phase viscous fluids or complex fluids, we introduce two new, *explicit*, convective velocities $u_\star^n$ and $u_{\star\star}^n$ in the phase equations. $u_\star^n$ and $u_{\star\star}^n$ can be computed directly from (2.27) and (2.29), i.e.,

$$
u_\star^n = \left(I + \frac{\delta t}{M_1}(\nabla\phi^n)^T\nabla\phi^n\right)^{-1}\left(u^n - \frac{1}{M_1}(\phi^{n+1} - \phi^n)\nabla\phi^n\right), \quad (2.32)
$$

$$
u_{\star\star}^n = \left(I + \frac{\delta t}{M_2}(\nabla\boldsymbol{d}^n)^T\nabla\boldsymbol{d}^n\right)^{-1}\left(u_\star^n - \frac{1}{M_2}(\boldsymbol{d}^{n+1} - \boldsymbol{d}^n)\nabla\boldsymbol{d}^n\right). \quad (2.33)
$$

It is easy to get $det(I + c(\nabla\phi)^T\nabla\phi) = 1 + c\nabla\phi\cdot\nabla\phi$, thus the above matrix is invertible.

- The scheme (2.26)-(2.31) is a totally decoupled, linear scheme. Indeed, (2.26), (2.28) and (2.30) are respectively (decoupled) linear elliptic equations for ϕ^{n+1}, $\boldsymbol{d}^{n+1}$ and $\tilde{u}^{n+1}$, and (2.31) can be restated as a Poisson equation for $p^{n+1} - p^n$.

Therefore, at each time step, one only needs to solve a sequence of decoupled elliptic equations which can be solved very efficiently.

- As we shall show below, the above scheme is unconditionally energy stable.

Theorem 2.3.1. *Under the condition* (2.19), *and* $S \geq \frac{\lambda \eta L}{2}$, *the scheme* (2.26)-(2.31) *admits a unique solution satisfying the following discrete energy dissipation law:*

$$E^{n+1} + \frac{\delta t^2}{2}\|\nabla p^{n+1}\|^2 + \left\{ \nu \delta t \|\nabla \tilde{u}^{n+1}\|^2 + \delta t \left(\frac{|\dot{\phi}^{n+1}|^2}{M_1} + \frac{|\dot{\boldsymbol{d}}^{n+1}|^2}{M_2} \right) \right\} \leq E^n + \frac{\delta t^2}{2}\|\nabla p^n\|^2,$$

where

$$E^n = \frac{1}{2}\|u^n\|^2 + \lambda \left(\eta \left(\frac{\|\nabla \boldsymbol{d}^n\|^2}{2} + (\mathbf{G}(\boldsymbol{d}^n), 1) \right) + \frac{1}{\eta} \frac{\|\boldsymbol{d}^n - \nabla \phi^n\|^2}{2} - \frac{\tau}{2}\|\boldsymbol{d}^n \cdot \boldsymbol{\mu}_1\|^2 \right) \quad (2.34)$$

Proof. From the definition of $u_\star^n$ and $u_{\star\star}^n$ in (2.27) and (2.29), we can rewrite the momentum equation (2.30) as follows

$$\frac{\tilde{u}^{n+1} - u_{\star\star}^n}{\delta t} + (u^n \cdot \nabla)\tilde{u}^{n+1} - \mu_4 \Delta \tilde{u}^{n+1} + \nabla p^n = 0. \quad (2.35)$$

By taking the inner product of (2.35) with $2\delta t \tilde{u}^{n+1}$, and using the identity

$$(a - b, 2a) = |a|^2 - |b|^2 + |a - b|^2, \quad (2.36)$$

we obtain

$$\|\tilde{u}^{n+1}\|^2 - \|u_{\star\star}^n\|^2 + \|\tilde{u}^{n+1} - u_{\star\star}^n\|^2 + 2\mu_4 \delta t \|\nabla \tilde{u}^{n+1}\|^2 + 2\delta t (\nabla p^n, \tilde{u}^{n+1}) = 0. \quad (2.37)$$

To deal with the pressure term, we take the inner product of (2.31) with $2\delta t^2 \nabla p^n$ to derive

$$\delta t^2 (\|\nabla p^{n+1}\|^2 - \|\nabla p^n\|^2 - \|\nabla p^{n+1} - \nabla p^n\|^2) = 2\delta t (\tilde{u}^{n+1}, \nabla p^n). \quad (2.38)$$

By taking the inner product of (2.31) with u^{n+1}, we obtain

$$\|u^{n+1}\|^2 + \|u^{n+1} - \tilde{u}^{n+1}\|^2 = \|\tilde{u}^{n+1}\|^2. \quad (2.39)$$

42

We also derive from (2.31) directly that

$$\delta t^2 \|\nabla p^{n+1} - \nabla p^n\|^2 = \|\tilde{u}^{n+1} - u^{n+1}\|^2. \tag{2.40}$$

Combining all identities above, we obtain

$$\|u^{n+1}\|^2 - \|u_{\star\star}^n\|^2 + \|\tilde{u}^{n+1} - u_{\star\star}^n\|^2$$
$$+ \delta t^2 (\|\nabla p^{n+1}\|^2 - \|\nabla p^n\|^2) + 2\nu\delta t\|\nabla\tilde{u}^{n+1}\|^2 = 0. \tag{2.41}$$

Next, we derive from (2.27) and (2.29) that

$$\frac{u_\star^n - u^n}{\delta t} = -\frac{\dot{\phi}^{n+1}}{M_1}\nabla\phi^n, \tag{2.42}$$

$$\frac{u_{\star\star}^n - u_\star^n}{\delta t} = -\frac{\dot{\boldsymbol{d}}^{n+1}}{M_2}\nabla\boldsymbol{d}^n. \tag{2.43}$$

By taking the inner product of (2.42) with $2\delta t u_\star^n$, of (2.43) with $2\delta t u_{\star\star}^n$, we obtain

$$\|u_\star^n\|^2 - \|u^n\|^2 + \|u_\star^n - u_n\|^2 = -2\delta t(\frac{\dot{\phi}^{n+1}}{M_1}\nabla\phi^n, u_\star^n), \tag{2.44}$$

$$\|u_{\star\star}^n\|^2 - \|u_\star^n\|^2 + \|u_{\star\star}^n - u_\star^n\|^2 = -2\delta t(\frac{\dot{\boldsymbol{d}}^{n+1}}{M_2}\nabla\boldsymbol{d}^n, u_{\star\star}^n). \tag{2.45}$$

Then, by taking the inner product of (2.26) with $2(\phi^{n+1} - \phi^n)$, we obtain

$$2\delta t\frac{\|\dot{\phi}^{n+1}\|^2}{M_1} - 2\delta t(\frac{\dot{\phi}^{n+1}}{M_1}, (u_\star^n \cdot \nabla)\phi^n) + \frac{2\lambda}{\eta}\left(\nabla \cdot \boldsymbol{d}^n, \phi^{n+1} - \phi^n\right)$$
$$+ \frac{\lambda}{\eta}\left(\|\nabla\phi^{n+1}\|^2 - \|\nabla\phi^n\|^2 + \|\nabla\phi^{n+1} - \nabla\phi^n\|^2\right) \tag{2.46}$$
$$= 0.$$

By taking the inner product of (2.28) with $2(\boldsymbol{d}^{n+1} - \boldsymbol{d}^n)$, we arrive at

$$2S\|\boldsymbol{d}^{n+1} - \boldsymbol{d}^n\|^2 + 2\delta t\frac{\|\dot{\boldsymbol{d}}^{n+1}\|^2}{M_2} - 2\delta t(\frac{\dot{\boldsymbol{d}}^{n+1}}{M_2}, (u_{\star\star}^n \cdot \nabla)\boldsymbol{d}^n)$$
$$+ 2\lambda\eta\left(\frac{\|\nabla\boldsymbol{d}^{n+1}\|^2}{2} - \frac{\|\nabla\boldsymbol{d}^n\|^2}{2} + \frac{\|\nabla\boldsymbol{d}^{n+1} - \nabla\boldsymbol{d}^n\|^2}{2}\right)$$
$$+ \frac{\lambda}{\eta}\left(\|\boldsymbol{d}^{n+1}\|^2 - \|\boldsymbol{d}^n\|^2 + \|\boldsymbol{d}^{n+1} - \boldsymbol{d}^n\|^2\right) \tag{2.47}$$
$$+ 2\lambda\eta(\boldsymbol{g}(\boldsymbol{d}^n), \boldsymbol{d}^{n+1} - \boldsymbol{d}^n) - \frac{2\lambda}{\eta}\left(\nabla\phi^{n+1}, \boldsymbol{d}^{n+1} - \boldsymbol{d}^n\right)$$
$$- 2\lambda\tau\left((\boldsymbol{d}^n \cdot \boldsymbol{\mu}_1)\boldsymbol{\mu}_1, \boldsymbol{d}^{n+1} - \boldsymbol{d}^n\right)$$
$$= 0.$$

Combining (2.41), (2.44), (2.45), (2.46), and (2.47), we arrive at

$$
\|u^{n+1}\|^2 - \|u^n\|^2 + \|\tilde{u}^{n+1} - u_{\star\star}^n\|^2 + \|u_{\star\star}^n - u_\star^n\|^2 + \|u_\star^n - u^n\|^2
$$

$$
+ \delta t^2 (\|\nabla p^{n+1}\|^2 - \|\nabla p^n\|^2)
$$

$$
+ 2\nu\delta t\|\nabla\tilde{u}^{n+1}\|^2 + 2\delta t\frac{\|\dot{\phi}^{n+1}\|^2}{M_1} + 2\delta t\frac{\|\dot{d}^{n+1}\|^2}{M_2}
$$

$$
+ 2\lambda\eta\Big(\frac{\|\nabla d^{n+1}\|^2}{2} - \frac{\|\nabla d^n\|^2}{2} + \frac{\|\nabla d^{n+1} - \nabla d^n\|^2}{2}\Big)
$$

$$
+ \frac{\lambda}{\eta}(\|d^{n+1}\|^2 - \|d^n\|^2 + \|d^{n+1} - d^n\|^2)
$$

$$
+ \frac{\lambda}{\eta}(\|\nabla\phi^{n+1}\|^2 - \|\nabla\phi^n\|^2 + \|\nabla\phi^{n+1} - \nabla\phi^n\|^2)
\tag{2.48}
$$

$$
+ 2S\|d^{n+1} - d^n\|^2
$$

$$
+ 2\lambda\eta(g(d^n), d^{n+1} - d^n) \qquad\qquad (\text{:Term } A)
$$

$$
+ \frac{2\lambda}{\eta}(\nabla\cdot d^n, \phi^{n+1} - \phi^n) - \frac{2\lambda}{\eta}(\nabla\phi^{n+1}, d^{n+1} - d^n) \quad (\text{:Term } B)
$$

$$
- 2\lambda\tau\Big((d^n\cdot\mu_1)\mu_1, d^{n+1} - d^n\Big) \qquad\qquad (\text{:Term } C)
$$

$$
= 0.
$$

We deal with the terms A, B, C as follows.

For Term A, we apply the Taylor expansions to obtain

$$
A = 2\lambda\eta(\mathbf{G}(d^{n+1}) - \mathbf{G}(d^n), 1) - 2\lambda\eta\Big(\frac{g_1'(\xi)}{2}, |d^{n+1} - d^n|^2\Big).
\tag{2.49}
$$

For Term B, we have

$$
B = -2\frac{\lambda}{\eta}\Big((d^n, \nabla\phi^{n+1} - \nabla\phi^n) + (d^{n+1} - d^n, \nabla\phi^{n+1})\Big)
$$

$$
= -2\frac{\lambda}{\eta}\Big((d^{n+1}, \nabla\phi^{n+1}) - (d^n, \nabla\phi^n)\Big).
\tag{2.50}
$$

For Term C, we have

$$
C = -2\lambda\tau\Big((d^n\cdot\mu_1), (d^{n+1}\cdot\mu_1) - (d^n\cdot\mu_1)\Big)
$$

$$
= -\lambda\tau\Big(\|d^{n+1}\cdot\mu_1\|^2 - \|d^n\cdot\mu_1\|^2 - \|(d^{n+1} - d^n)\cdot\mu_1\|^2\Big).
\tag{2.51}
$$

By combining (2.48), (2.49), (2.50) and (2.51), we have

$$
\|u^{n+1}\|^2 - \|u^n\|^2 + \|\tilde{u}^{n+1} - u_{\star\star}^n\|^2 + \|u_{\star\star}^n - u_{\star}^n\|^2 + \|u_{\star}^n - u^n\|^2
$$

$$
+ \delta t^2 (\|\nabla p^{n+1}\|^2 - \|\nabla p^n\|^2)
$$

$$
+ 2\nu\delta t\|\nabla\tilde{u}^{n+1}\|^2 + 2\delta t\frac{\|\dot{\phi}^{n+1}\|^2}{M_1} + 2\delta t\frac{\|\dot{\boldsymbol{d}}^{n+1}\|^2}{M_2}
$$

$$
+ 2\lambda\eta\Big(\frac{\|\nabla\boldsymbol{d}^{n+1}\|^2}{2} - \frac{\|\nabla\boldsymbol{d}^n\|^2}{2} + \frac{\|\nabla\boldsymbol{d}^{n+1} - \nabla\boldsymbol{d}^n\|^2}{2}\Big)
$$

$$
+ 2\lambda\eta(\mathbf{G}(\boldsymbol{d}^{n+1}) - \mathbf{G}(\boldsymbol{d}^n), 1)
$$

$$
+ \frac{\lambda}{\eta}(\|\boldsymbol{d}^{n+1}\|^2 - \|\boldsymbol{d}^n\|^2 + \|\boldsymbol{d}^{n+1} - \boldsymbol{d}^n\|^2)
$$

$$
+ \frac{\lambda}{\eta}(\|\nabla\phi^{n+1}\|^2 - \|\nabla\phi^n\|^2 + \|\nabla\phi^{n+1} - \nabla\phi^n\|^2) \tag{2.52}
$$

$$
- 2\frac{\lambda}{\eta}\Big((\boldsymbol{d}^{n+1}, \nabla\phi^{n+1}) - (\boldsymbol{d}^n, \nabla\phi^n)\Big)
$$

$$
- \lambda\tau\Big(\|\boldsymbol{d}^{n+1}\cdot\boldsymbol{\mu}_1\|^2 - \|\boldsymbol{d}^n\cdot\boldsymbol{\mu}_1\|^2\Big)
$$

$$
+ (2S - \lambda\eta L)\|\boldsymbol{d}^{n+1} - \boldsymbol{d}^n\|^2
$$

$$
+ \lambda\tau\|(\boldsymbol{d}^{n+1} - \boldsymbol{d}^n)\cdot\boldsymbol{\mu}_1\|^2
$$

$$
= 0.
$$

Finally, we obtain the desired result after dropping some positive terms. □

2.4 NUMERICAL SIMULATIONS

We now present some 2D numerical experiments to demonstrate the efficiency, stability and accuracy of the propose numerical scheme (2.26)-(2.31). The computatational domain is $(x, y) \in [0, 2\ell] \times [0, 2]$. For x-axis, we set the periodic boundary condition, and for $y-$ axis, we set Neumann or Dirichelet boundary conditions. We adopt the second order central finite difference method to discretize the space. The magnectic field is always set as $\boldsymbol{\mu}_1 = (0, 1)$. If not explicitly specified, the default values of order parameters are given as follows,

$$
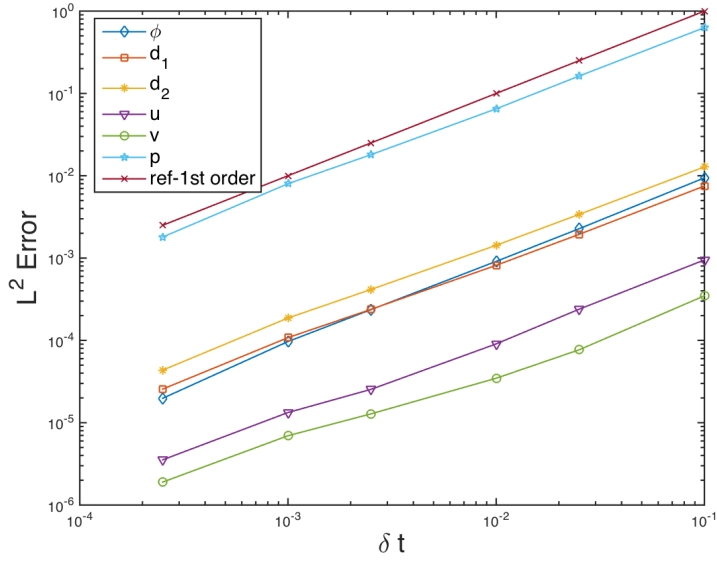\ell = 2, \epsilon = 0.02, \eta = 0.02, M_1 = 0.08, M_2 = 2, \lambda = 2.5, \tau = 16. \tag{2.53}
$$

Figure 2.1: The L^2 errors of the layer funciton ϕ, the director field $\boldsymbol{d} = (d_1, d_2)$, the velocity $u = (u, v)$ and pressure p. The slopes show that the scheme is asymptotically first-order accurate in time.

2.4.1 ACCURACY TEST

We first test the convergence rate of scheme (2.26)-(2.31). We set the following initial conditions as

$$\begin{cases} \boldsymbol{d}(t = 0) = (sin(\pi x)cos(\pi y), cos(\pi x)cos(\pi y)), \\ \phi(t = 0) = cos(\pi y), \\ (u(t = 0), p(t = 0)) = (0, 0). \end{cases} \quad (2.54)$$

The boundary conditions are Neumann type along y-axis (cf. (2.15)). We use 128×128 grid points to discretize the space, and perform the mesh refinement test for time. We choose the numerical solution with the time step size $\delta t = 1 \times 10^{-4}$ as the benchmark solution (approximate exact solution) for computing errors. Figure 2.1 plots the L^2 errors for various time step sizes. We observe that the scheme is asymptotically first-order accurate in time for all variables as expected.

46

2.4.2 Chevron pattern induced by the magnetic force

We now consider the effects from the magnetic force for the no flow case ($u = 0$). Initially, a smectic A liquid crystal is confined between two flat parallel plates and uniformly aligned in a way that the smectic layers are parallel to the bounding plates and the directors are aligned homeotropically, that is, perpendicular to the smectic layers. A magnetic field is applied in the direction parallel to the smectic layers, which induce the layer undulation (chevron pattern) phenomena. The initial conditions read as follows.

$$\begin{aligned} \boldsymbol{d}(t=0) &= (0,1) + 0.001(\mathrm{r}and(x,y), \mathrm{r}and(x,y)), \\ \phi(t=0) &= y, \end{aligned} \tag{2.55}$$

where the $\mathrm{r}and(x,y)$ is the small perturbation that is the random number in $[-1, 1]$ and has zero mean. We set the Dirichlet type boundary condition for ϕ and $\boldsymbol{d}$ as follows,

$$\boldsymbol{d}|_{y=\pm 1} = (0,1),\ \phi|_{y=1} = 1,\ \phi|_{y=-1} = -1. \tag{2.56}$$

We take $\delta t = 0.001$ to obtain better accuracy. Fig. 2.2 shows the snapshots of the layer function ϕ at $t = 0, 0.2, 0.4$ and 0.8. Initially at $t = 0$, the layer function take the linear profile along the $y-$ axis. When time evolves, we observe some undulations appear at $t = 0.2$. The layer function quickly reaches the steady solution at $t = 0.8$ with the saw tooth shape. This undulation phenomenon is called the Helfrich-Hurault effect (cf. [34, 38]). Fig. 2.3 shows the snapshots of the directior field $\boldsymbol{d}$. The numerical solution presents similar features to those obtained in [42]. We also plot the energy dissipative curve in Fig. 2.4, which confirms that our algorithm is energy stable.
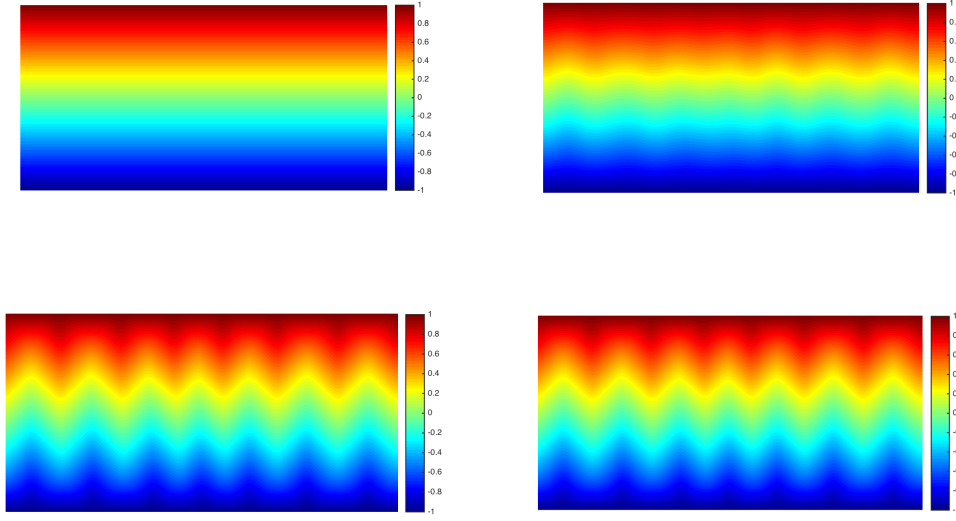
Figure 2.2: Snapshots of the layer function ϕ are taken at $t = 0$, 0.2, 0.4 and 0.8 for Example 2.4.2.

2.4.3 CHEVRON PATTERN INDUCED BY MAGNETIC FORCE AND SHEAR FLOW

We now impose the shear flow on the top and bottom plates to see how the flow affects the undulation. The initial and boundary conditions of ϕ and $\boldsymbol{d}$ are same as the example 2.4.2. For velocity and pressure, the initial and boundary conditions are:

$$u(t = 0) = (10(y - 1), 0),\ p(t = 0) = 0$$
$$u|_{y=1} = (10, 0), u|_{y=-1} = (-10, 0). \tag{2.57}$$

Fig. 2.5 show the snapshots of the layer function ϕ at $t = 0, 0.3, 0.4, 0.5, 0.6$ and 0.8. When time evolves, the layer undulations still appear but the symmetry is largely disturbed by the shear flow. Fig. 2.6 shows the snapshots of the directior field $\boldsymbol{d}$. We also plot the first component of the velocity field $u = (u, v)$ in Fig. 2.7, where the linear profile is deformed to show nonlinearility.

48
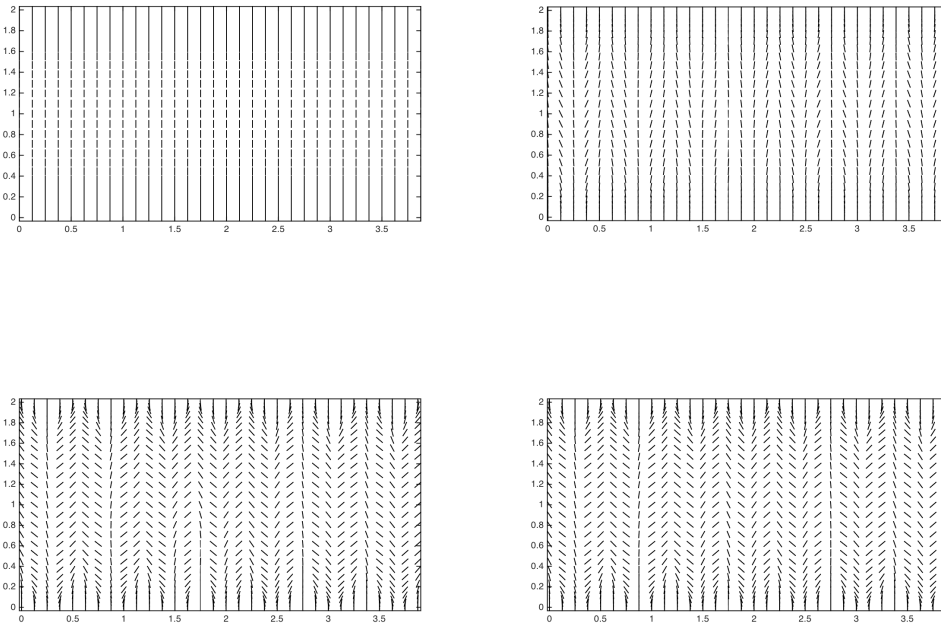
Figure 2.3: Snapshots of the director field $\boldsymbol{d}$ are taken at $t = 0$, 0.2, 0.4 and 0.8 for Example 2.4.2.
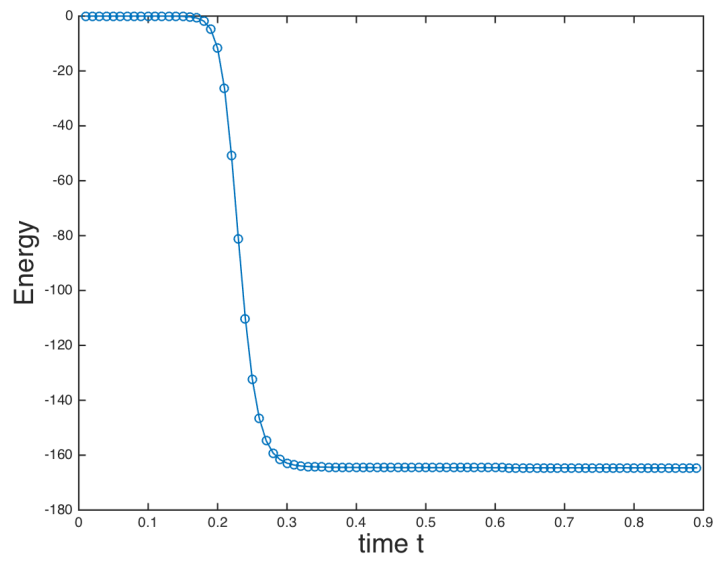

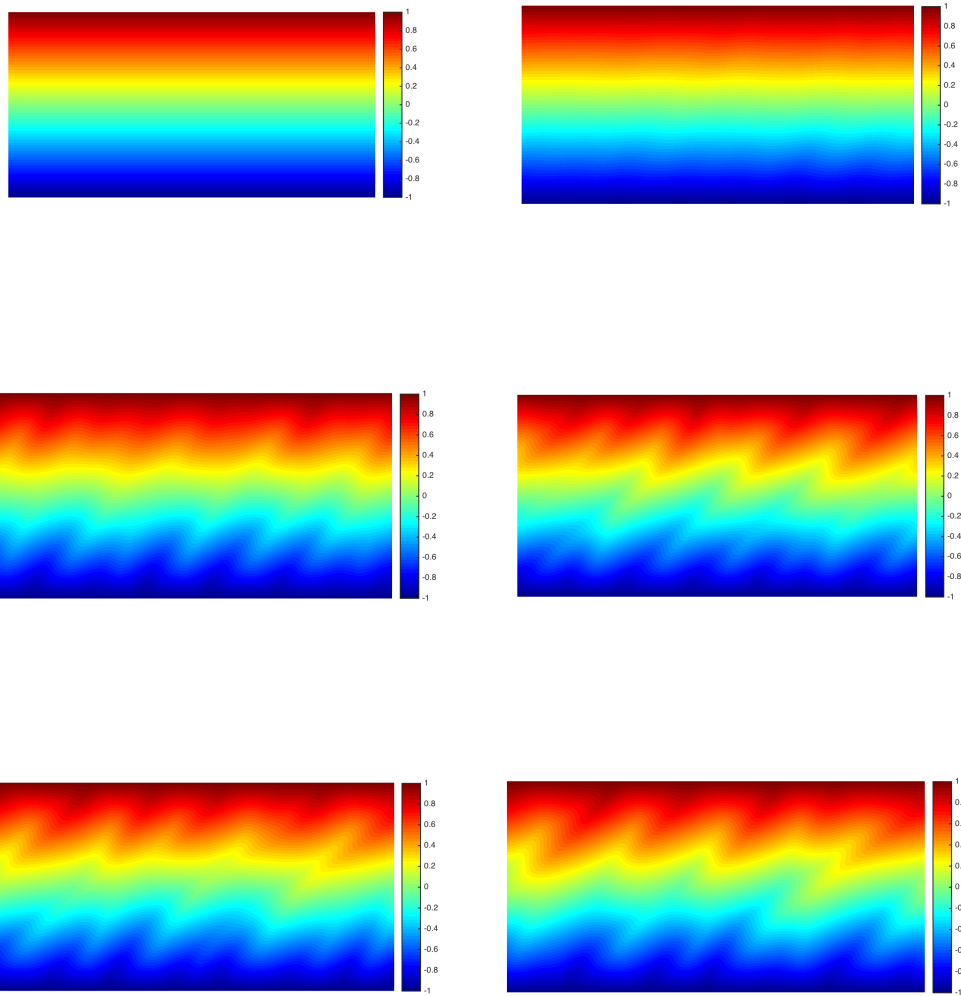Figure 2.4: Time evolution of the free energy functional of Example 2.4.2.

Figure 2.5: Snapshots of the layer function ϕ are taken at $t = 0$, 0.3, 0.4 , 0.5, 0.6 and 0.8 for Example 2.4.3.
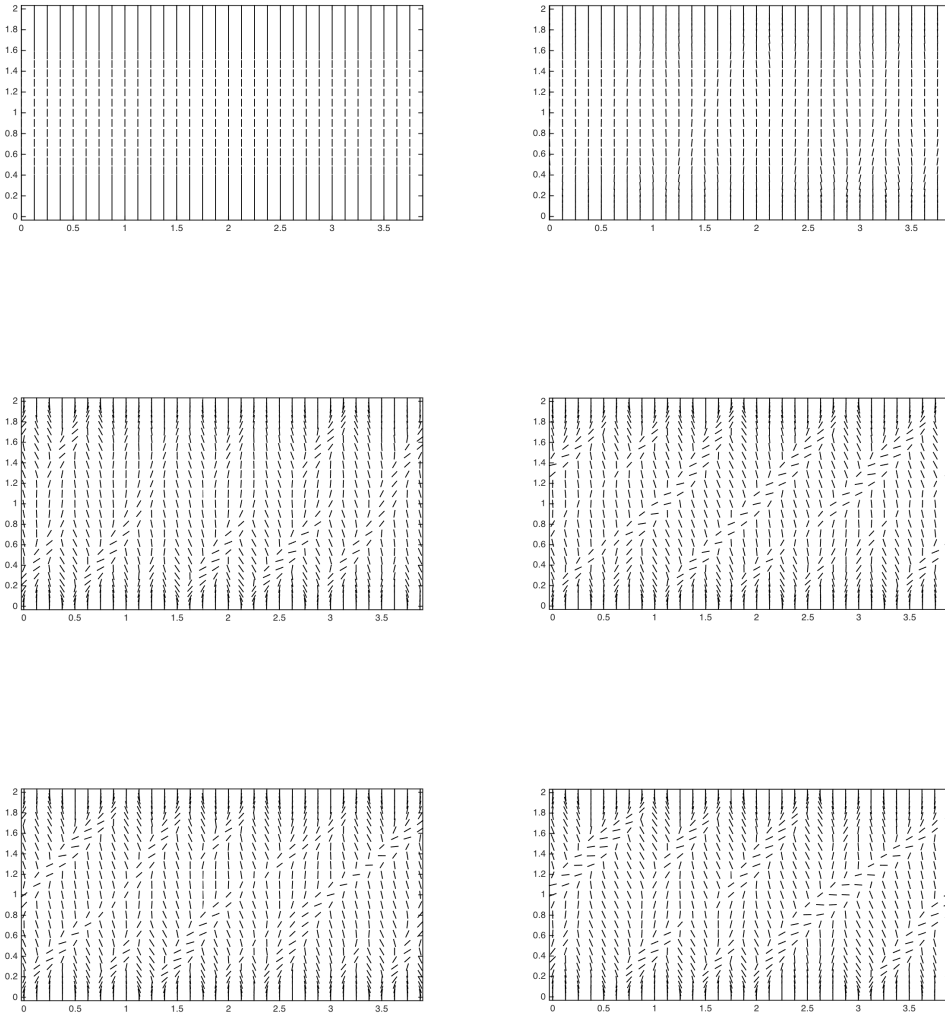
Figure 2.6: Snapshots of the director field $\boldsymbol{d}$ are taken at $t = 0$, 0.3, 0.4 , 0.5, 0.6 and 0.8 for Example 2.4.3.
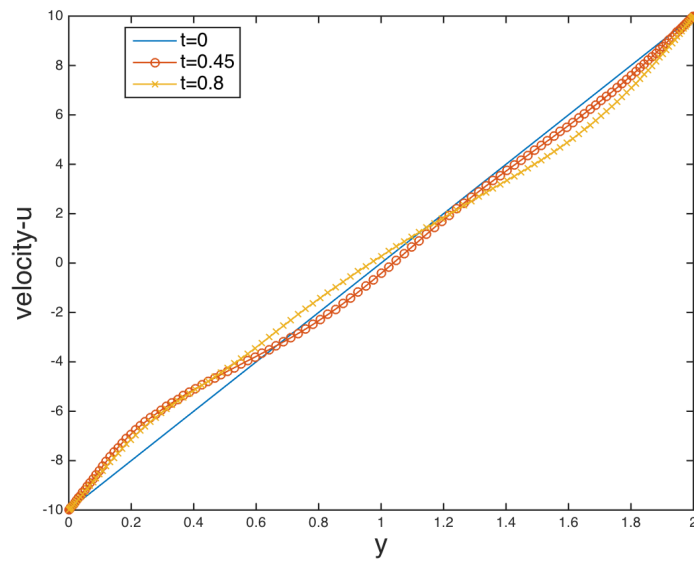
Figure 2.7: Snapshots of the profile for the first component $u(y)$ of the velocity field $u = (u, v)$ at the center $(x = 2)$ and $t = 0, 0.45$ and 0.8.

Bibliography

[1] D. N. Arnold, F. Brezzi, and M. Fortin. "A stable finite element for the Stokes equations". In: *Calcolo* 21.4 (1984), 337–344 (1985). ISSN: 0008-0624. DOI: 10.1007/BF02576171. URL: http://dx.doi.org/10.1007/BF02576171.

[2] A. Baskaran et al. "Convergence analysis of a second order convex splitting scheme for the modified phase field crystal equation". In: *SIAM J. Numer. Anal.* 51.5 (2013), pp. 2851–2873. ISSN: 0036-1429. DOI: 10.1137/120880677. URL: http://dx.doi.org/10.1137/120880677.

[3] Franck Boyer and Sebastian Minjeaud. "Numerical schemes for a three component Cahn-Hilliard model". In: *ESAIM Math. Model. Numer. Anal.* 45.4 (2011), pp. 697–738. ISSN: 0764-583X. DOI: 10.1051/m2an/2010072. URL: http://dx.doi.org/10.1051/m2an/2010072.

[4] A. Bray. "Theory of phase-ordering kinetics". In: *Adv. Phys.* ().

[5] David L. Brown, Ricardo Cortez, and Michael L. Minion. "Accurate projection methods for the incompressible Navier-Stokes equations". In: *J. Comput. Phys.* 168.2 (2001), pp. 464–499. ISSN: 0021-9991. DOI: 10.1006/jcph.2001.6715. URL: http://dx.doi.org/10.1006/jcph.2001.6715.

[6] G. Caginalp and X. Chen. "Convergence of the phase field model to its sharp interface limits". In: *Euro. Jnl of Applied Mathematics* 9 (1998), pp. 417–445.

[7] J. W. Cahn and J. E. Hilliard. "Free energy of a nonuniform system. I. Interfacial free energy." In: *J. Chem. Phys.* 28 (1958), pp. 258–267.

[8] John W. Cahn. "Free Energy of a Nonuniform System. II. Thermodynamic Basis". In: *Journal of Chemical Physics* 30.5 (1959).

[9] John W. Cahn and John E. Hilliard. "Free Energy of a Nonuniform System. I. Interfatial Free Energy". In: *Journal of Chemical Physics* 28.2 (1958).

[10] P. M. Chaikin and T. C. Lubensky. "Principles of Condensed Matter Physics". In: *Cambridge* (1995).

[11]   S Chandrasekhar. "Liquid Crystals (2nd ed.). Cambridge: Cambridge University Press, ISBN 0-521-41747-3". In: (1992).

[12]   J. Chen and T. C. Lubensky. "Landau-Ginzburg mean-field theory for the nematic to smectic-C and nematic to smectic-A phase transitions." In: *Phys. Rev. A*. 14 (1976), pp. 1202–1207.

[13]   L.Q. Chen and Jie Shen. "Applications of semi-implicit Fourier-spectral method to phase field equations". In: *Computer Physics Communications* 108.2-3 (1998), pp. 147 –158. ISSN: 0010-4655. DOI: `http://dx.doi.org/10.1016/S0010-4655(97)00115-X`. URL: `http://www.sciencedirect.com/science/article/pii/S001046559700115X`.

[14]   Philippe G. Ciarlet. *The finite element method for elliptic problems*. Vol. 40. Classics in Applied Mathematics. Philadelphia, PA: Society for Industrial and Applied Mathematics (SIAM), 2002, pp. xxviii+530. ISBN: 0-89871-514-8.

[15]   Craig Collins, Jie Shen, and Steven M. Wise. "An efficient, energy stable scheme for the Cahn-Hilliard-Brinkman system". In: *Commun. Comput. Phys.* 13.4 (2013), pp. 929–957. ISSN: 1815-2406.

[16]   N. Condette, C. Melcher, and E. Süli. "Spectral approximation of pattern-forming nonlinear evolution equations with double-well potentials of quadratic growth". In: *to appear in Math. Comp.* ().

[17]   S. Dong and J. Shen. "A time-stepping scheme involving constant coefficient matrices for phase-field simulations of two-phase incompressible flows with large density ratios". In: *Journal of Computational Physics* 231.17 (2012), pp. 5788 –5804. ISSN: 0021-9991. DOI: `10.1016/j.jcp.2012.04.041`. URL: `http://www.sciencedirect.com/science/article/pii/S0021999112002239`.

[18]   Qiang Du, Chun Liu, and Xiaoqiang Wang. "A phase field approach in the numerical study of the elastic bending energy for vesicle membranes". In: *Journal of Computational Physics* 198 (2004), pp. 450–468.

[19]   Weinan E. "Nonlinear continuum theory of Smectic-A liquid crystals". In: *Arch. Ration. Mech. Anal.* 137 (1997), pp. 159–175.

[20]   Weinan E and Jian-Guo Liu. "Projection method. I. Convergence and numerical boundary layers". In: *SIAM J. Numer. Anal.* 32.4 (1995), pp. 1017–1057. ISSN: 0036-1429. DOI: `10.1137/0732047`. URL: `http://dx.doi.org/10.1137/0732047`.

[21]   K. R. Elder et al. "Sharp interface limits of phase-field models". In: *Phys. Rev. E*. 64 (2001), p. 021604.

[22] David J. Eyre. "Unconditionally gradient stable time marching the Cahn-Hilliard equation". In: *Computational and mathematical models of microstructural evolution (San Francisco, CA, 1998)*. Vol. 529. Mater. Res. Soc. Sympos. Proc. Warrendale, PA: MRS, 1998, pp. 39–46.

[23] David J. Eyre. "Unconditionally gradient stable time marching the Cahn-Hilliard equation". In: *Computational and mathematical models of microstructural evolution (San Francisco, CA, 1998)*. Vol. 529. Mater. Res. Soc. Sympos. Proc. Warrendale, PA: MRS, 1998, pp. 39–46.

[24] A. Fick. "Poggendorff's Annalen." In: *Journal of the american mathematics society* (1855), pp. 59–86.

[25] Giordano Tierra Francisco Guillen-Gonzaleza. "Approximation of Smectic-A liquid crystals". In: *Comput. Methods Appl. Mech. Engrg.* 290 (2015), pp. 342–361.

[26] P. G. de Gennes and J. Prost. *The Physics of Liquid Crystals*. Oxford University Press, 1993.

[27] J. L. Guermond, P. Minev, and J. Shen. "An Overview of Projection methods for incompressible flows". In: *Comput. Methods Appl. Mech. Engrg.* 195 (2006), pp. 6011–6045.

[28] J.-L. Guermond and L. Quartapelle. "On stability and convergence of projection methods based on pressure Poisson equation". In: *Internat. J. Numer. Methods Fluids* 26.9 (1998), pp. 1039–1053. ISSN: 0271-2091. DOI: 10.1002/(SICI)1097-0363(19980515)26:9<1039::AID-FLD675>3.0.CO;2-U. URL: http://dx.doi.org.proxy.lib.fsu.edu/10.1002/(SICI)1097-0363(19980515)26:9<1039::AID-FLD675>3.0.CO;2-U.

[29] J.-L. Guermond and L. Quartapelle. "On the approximation of the unsteady Navier-Stokes equations by finite element projection methods". In: *Numer. Math.* 80.2 (1998), pp. 207–238. ISSN: 0029-599X. DOI: 10.1007/s002110050366. URL: http://dx.doi.org/10.1007/s002110050366.

[30] J. L. Guermond and Jie Shen. "Velocity-correction projection methods for incompressible flows". In: *SIAM J. Numer. Anal.* 41.1 (2003), 112–134 (electronic). ISSN: 0036-1429. DOI: 10.1137/S0036142901395400. URL: http://dx.doi.org/10.1137/S0036142901395400.

[31] F. Guillén-González and G. Tierra. "On linear schemes for a Cahn-Hilliard diffuse interface model". In: *J. Comput. Phys.* 234 (2013), pp. 140–171. ISSN: 0021-9991. DOI: 10.1016/j.jcp.2012.09.020. URL: http://dx.doi.org.proxy.lib.fsu.edu/10.1016/j.jcp.2012.09.020.

[32] Daozhi Han and Xiaoming Wang. "A second order in time, uniquely solvable, unconditionally stable numerical scheme for Cahn–Hilliard–Navier–Stokes equation". In: *J. Comput. Phys.* 290 (2015), pp. 139–156. ISSN: 0021-9991. DOI: 10.1016/j.jcp.2015.02.046. URL: http://dx.doi.org/10.1016/j.jcp.2015.02.046.

[33] F. Hecht. "New development in freefem++". In: *J. Numer. Math.* 20.3-4 (2012), pp. 251–265. ISSN: 1570-2820.

[34] W. Helfrich. "Electrohydrodynamic and dielectric instabilities of cholesteric liquid crystals". In: *The Journal of Chemical Physics* 55 (1971), pp. 839–842.

[35] Z. Hu et al. "Stable and efficient finite-difference nonlinear-multigrid schemes for the phase field crystal equation". In: *J. Comput. Phys.* 228.15 (2009), pp. 5323–5339. ISSN: 0021-9991. DOI: 10.1016/j.jcp.2009.04.020. URL: http://dx.doi.org/10.1016/j.jcp.2009.04.020.

[36] J. Hua et al. "Energy law preserving C0 finite element schemes for phase field models in two-phase flow computations". In: *J. of Comput. Phys.* 230 (2011), pp. 7155–7131.

[37] Jinsong Hua et al. "Energy law preserving C0 finite element schemes for phase field models in two-phase flow computations". In: *Journal of Computational Physics* 230.19 (2011), pp. 7115 –7131. ISSN: 0021-9991. DOI: 10.1016/j.jcp.2011.05.013. URL: http://www.sciencedirect.com/science/article/pii/S0021999111003172.

[38] J. P. Hurault. "Static distortions of a cholesteric planar structure induced by magnetic or ac electric fields". In: *The Journal of Chemical Physics* 59 (1973), pp. 2068–2075.

[39] Ross Ingram. "A new linearly extrapolated Crank-Nicolson time-stepping scheme for the Navier-Stokes equations". In: *Math. Comp.* 82.284 (2013), pp. 1953–1973. ISSN: 0025-5718. DOI: 10.1090/S0025-5718-2013-02678-6. URL: http://dx.doi.org.proxy.lib.fsu.edu/10.1090/S0025-5718-2013-02678-6.

[40] X. L. Li J. Glimm J. W. Grove and D. C. Tan. "Robust computational algorithms for dynamic interface tracking in three dimensions". In: *SIAM J. Sci. Comput.* 21 (2000), pp. 2240–2256.

[41] Y. Liu J. Glimm X. L. Li and N. Zhao. "Conservative front tracking and level set algorithms". In: *Proc. Natl. Acad. Sci. USA* 98 (2001), pp. 14198–14201.

[42] S. Joo and D. Phillips. "The phase transitions from chiral nematic toward smectic liquid crystals." In: *Communications in Mathematical Physics* 269 (2007), pp. 367–399.

[43] J. van Kan. "A second-order accurate pressure-correction scheme for viscous incompressible flow". In: *SIAM J. Sci. Statist. Comput.* 7.3 (1986), pp. 870–891. ISSN: 0196-5204. DOI: 10.1137/0907059. URL: http://dx.doi.org/10.1137/0907059.

[44] David Kay, Vanessa Styles, and Richard Welford. "Finite element approximation of a Cahn-Hilliard-Navier-Stokes system". In: *Interfaces Free Bound.* 10.1 (2008), pp. 15–43. ISSN: 1463-9963. DOI: 10.4171/IFB/178. URL: http://dx.doi.org/10.4171/IFB/178.

[45] Daniel Kessler, Ricardo H. Nochetto, and Alfred Schmidt. "A posteriori error control for the Allen-Cahn problem: circumventing Gronwall's inequality". In: *M2AN Math. Model. Numer. Anal.* 38.1 (2004), pp. 129–142. ISSN: 0764-583X. DOI: 10.1051/m2an:2004006. URL: http://dx.doi.org/10.1051/m2an:2004006.

[46] Junseok Kim, Kyungkeun Kang, and John Lowengrub. "Conservative multigrid methods for Cahn-Hilliard fluids". In: *J. Comput. Phys.* 193.2 (2004), pp. 511–543. ISSN: 0021-9991. DOI: 10.1016/j.jcp.2003.07.035. URL: http://dx.doi.org/10.1016/j.jcp.2003.07.035.

[47] X. Hu L. Fu and N. Adams. "A family of high-order targeted ENO schmes for compressible-fluid simulations". In: *J. of Comput. Phys.* 305 (2016), pp. 333–359.

[48] J. Li and Y. Renardy. "Numerical Study of flows of two immiscible liquids at low reynolds number". In: *SIAM Review* 42 (2000), pp. 417–439.

[49] J. Li and Y. Renardy. "Shear-induced rupturing of a viscous drop in a bingham liquid". In: *J. Non-Newtonian Fluid Mech.* 95 (2000), pp. 235–251.

[50] F. H. Lin. "Mathematics theory of liquid crystals, in Applied Mathematics At The Turn Of Century: Lecture notes of the 1993 summer school, Universidat Complutense de Madrid". In: (1995).

[51] F. H. Lin. "On nematic liquid crystals with variable degree of orientation". In: *Communications on Pure and Applied Mathematics* 44 (1991), pp. 453–468.

[52] P. Lin and C. Liu. "Simulation of singularity dynamics in liquid crystal flows: a C0 finite element approach". In: *J. of Comput. Phys.* 215 (2006), pp. 348–362.

[53] C. Liu and J. Shen. "A phase field model for the mixture of two incompressible fluids and its approximation by a Fourier-spectral method". In: *Physica D* 179.3-4 (2003), pp. 211–228.

[54] C. Liu and N.J. Walkington. "An Eulerian description of fluids containing visco-hyperelastic particles". In: *Arch. Rat. Mech. Anal.* 159 (2001), pp. 229–252.

[55] Chun Liu and Jie Shen. "A phase field model for the mixture of two incompressible fluids and its approximation by a Fourier-spectral method". In: *Physica D: Nonlinear Phenomena* 179.34 (2003), pp. 211 –228. ISSN: 0167-2789. DOI: 10.1016/S0167-2789(03)00030-7. URL: http://www.sciencedirect.com/science/article/pii/S0167278903000307.

[56] Fei Liu and Jie Shen. "Stabilized semi-implicit spectral deferred correction methods for Allen-Cahn and Cahn-Hilliard equations". In: *Math. Methods Appl. Sci.* 38.18 (2015), pp. 4564–4575. ISSN: 0170-4214. DOI: 10.1002/mma.2869. URL: http://dx.doi.org/10.1002/mma.2869.

[57] A. Magni and G. Cottet. "Accurate, non-oscillatory, remeshing schemes for particle methods". In: *J. of Comput. Phys.* 231 (2012), pp. 152–172.

[58] S. Minjeaud. "An unconditionally stable uncoupled scheme for a triphasic Cahn-Hilliard/Navier-Stokes model." In: *Commun. Comput. Phys.* 29 (2013), pp. 584–618.

[59] Sebastian Minjeaud. "An unconditionally stable uncoupled scheme for a triphasic Cahn-Hilliard/Navier-Stokes model". In: *Numer. Methods Partial Differential Equations* 29.2 (2013), pp. 584–618. ISSN: 0749-159X. DOI: 10.1002/num.21721. URL: http://dx.doi.org/10.1002/num.21721.

[60] R. Strzodka N. Cuntz A. Kolb and D. Weiskopf. "Particle level set advection for the interactive visualization of unsteady 3D flow". In: *Computer Graphics Forum* 27 (2008), pp. 719–726.

[61] S. Osher and J. Sethian. "Fronts propagating with curvature dependent speed: Algorithms based on Hamilton Jacobi formulations". In: *J. of Comput. Phys.* 79 (1988), pp. 12–49.

[62] J. Shen and X. Yang. "A phase-field model and its numerical approximation for two-phase incompressible flows with different densities and viscositites". In: *SIAM J. Sci. Comput.* 32 (2010), pp. 1159–1179.

[63] J. Shen and X. Yang. "Energy Stable Schemes for Cahn-Hilliard phase-field model of two-phase incompressible flows". In: *Chinese Ann. Math. series B* 31 (2010), pp. 743–758.

[64] J. Shen and X. Yang. "Numerical Approximations of Allen-Cahn and Cahn-Hilliard Equations". In: *DCDS, Series A* 28 (2010), pp. 1169–1691.

[65] Jie Shen. "Modeling and numerical approximation of two-phase incompressible flows by a phase-field approach". In: *Multiscale modeling and analysis for materials simulation.* Vol. 22. Lect. Notes Ser. Inst. Math. Sci. Natl. Univ. Singap. World Sci. Publ., Hackensack, NJ, 2012, pp. 147–195.

[66] Jie Shen. "On error estimates of the projection methods for the Navier-Stokes equations: second-order schemes". In: *Math. Comp.* 65.215 (1996), pp. 1039–1065. ISSN: 0025-5718. DOI: `10.1090/S0025-5718-96-00750-8`. URL: `http://dx.doi.org/10.1090/S0025-5718-96-00750-8`.

[67] Jie Shen and Xiaofeng Yang. "A phase-field model and its numerical approximation for two-phase incompressible flows with different densities and viscosities". In: *SIAM J. Sci. Comput.* 32.3 (2010), pp. 1159–1179. ISSN: 1064-8275. DOI: `10.1137/09075860X`. URL: `http://dx.doi.org/10.1137/09075860X`.

[68] Jie Shen and Xiaofeng Yang. "An efficient moving mesh spectral method for the phase-field model of two-phase flows". In: *J. Comput. Phys.* 228.8 (2009), pp. 2978–2992. ISSN: 0021-9991. DOI: `10.1016/j.jcp.2009.01.009`. URL: `http://dx.doi.org/10.1016/j.jcp.2009.01.009`.

[69] Jie Shen and Xiaofeng Yang. "Decoupled energy stable schemes for phase field models of two phase incompressible flows". In: *SIAM Journal of Numerical Analysis* 53.1 (2015), pp. 279–296.

[70] Jie Shen and Xiaofeng Yang. "Numerical approximation of Allen-Cahn and Cahn-Hilliard equations". In: *Discrete and Continuous Dynamical Systems Series B* 28.4 (2010), pp. 1669–1691.

[71] Jie Shen et al. "Second-order convex splitting schemes for gradient flows with Ehrlich-Schwoebel type energy: application to thin film epitaxy". In: *SIAM J. Numer. Anal.* 50.1 (2012), pp. 105–125. ISSN: 0036-1429. DOI: `10.1137/110822839`. URL: `http://dx.doi.org/10.1137/110822839`.

[72] R. Témam. "Sur l'approximation de la solution des équations de Navier-Stokes par la méthode des pas fractionnaires. II". In: *Arch. Rational Mech. Anal.* 33 (1969), pp. 377–385. ISSN: 0003-9527.

[73] Roger Temam. *Navier-Stokes equations. Theory and numerical analysis.* Studies in Mathematics and its Applications, Vol. 2. Amsterdam: North-Holland Publishing Co., 1977, pp. x+500. ISBN: 0-7204-2840-8.

[74] C. Wang and S. M. Wise. "An energy stable and convergent finite-difference scheme for the modified phase field crystal equation". In: *SIAM J. Numer. Anal.* 49.3 (2011), pp. 945–969. ISSN: 0036-1429. DOI: 10.1137/090752675. URL: http://dx.doi.org/10.1137/090752675.

[75] Cheng Wang, Xiaoming Wang, and Steven M. Wise. "Unconditionally stable schemes for equations of thin film epitaxy". In: *Discrete Contin. Dyn. Syst.* 28.1 (2010), pp. 405–423. ISSN: 1078-0947. DOI: 10.3934/dcds.2010.28.405. URL: http://dx.doi.org/10.3934/dcds.2010.28.405.

[76] S. M. Wise. "Unconditionally stable finite difference, nonlinear multigrid simulation of the Cahn-Hilliard-Hele-Shaw system of equations". In: *J. Sci. Comput.* 44.1 (2010), pp. 38–68. ISSN: 0885-7474. DOI: 10.1007/s10915-010-9363-4. URL: http://dx.doi.org/10.1007/s10915-010-9363-4.

[77] X. Wu, G. J. van Zwieten, and K. G. van der Zee. "Stabilized second-order convex splitting schemes for Cahn-Hilliard models with application to diffuse-interface tumor-growth models". In: *Int. J. Numer. Methods Biomed. Eng.* 30.2 (2014), pp. 180–203. ISSN: 2040-7939. DOI: 10.1002/cnm.2597. URL: http://dx.doi.org/10.1002/cnm.2597.

[78] B. Merriman Y. C. Chang T. Y. Hou and S. Osher. "A level set formulation of eulerian interface capturing methods for incompressible fluid flows". In: *J. of Comput. Phys.* 124 (1996), pp. 449–464.

[79] Xiaofeng Yang et al. "Numerical simulations of jet pinching-off and drop formation using an energetic variational phase-field method". In: *J. Comput. Phys.* 218.1 (2006), pp. 417–428. ISSN: 0021-9991. DOI: 10.1016/j.jcp.2006.02.021. URL: http://dx.doi.org/10.1016/j.jcp.2006.02.021.

[80] Pengtao Yue et al. "A diffuse interface method for simulating two phase flows of complex fluids". In: *Journal of Fluid Mechanics* 515 (2004), pp. 293–317.